ABSTRACT

Title of Thesis: PATTERNS OF OYSTER NATURAL MORTALITY IN CHEAPEAKE BAY, MARYLAND DURING 1991-2017 AND ITS RELATIONSHIPS WITH ENVIRONMENTAL FACTORS AND DISEASE

Kathryn Leah Doering, Master of Science, 2019

Thesis Directed By: Professor Michael J. Wilberg,
Marine Estuarine Environmental Sciences

A common method of estimating natural mortality in bivalves includes several assumptions that are likely violated for oysters *Crassostrea virginica* in Chesapeake Bay, Maryland. In addition, while oyster disease dynamics are well studied spatially and temporally in the mid-Atlantic region, changes in disease-related relationships have not been investigated in Maryland. We developed a Bayesian estimator for natural mortality and applied it to oysters in Maryland. We then used the model output along with environmental factors and disease data to explore changes in the disease system over time. We found the largest differences in natural mortality estimates between the box count method and Bayesian model 1-3 years after a high mortality event. Some relationships changed over time in the disease system, most notably those associated with MSX, suggesting resistance to MSX has potentially developed. This work improves our estimates of natural mortality and understanding of oyster disease dynamics in Maryland.

PATTERNS OF OYSTER NATURAL MORTALITY IN CHEAPEAKE BAY, MARYLAND DURING 1991-2017 AND ITS RELATIONSHIPS WITH ENVIRONMENTAL FACTORS AND DISEASE

by

Kathryn Leah Doering

Thesis submitted to the Faculty of the Graduate School of the
University of Maryland, College Park, in partial fulfillment
of the requirements for the degree of
Master of Science
2019

Advisory Committee:
Professor Michael J. Wilberg, Chair
Associate Professor Lora A. Harris
Assistant Research Professor Dong Liang

Acknowledgements

Thanks to the Maryland Department of Natural Resources (MDNR) for collecting and providing the fall oyster dredge survey and disease data and to the Maryland Oyster Stock Assessment Team for sharing their knowledge of oysters in Maryland throughout the process of the stock assessment. Thanks specifically to Jodi Baxter, Christopher Dungan, Kelly Greenhawk, and Mitchell Tarnowski at MDNR for querying databases and providing information about the datasets.

Additional thanks to the Chesapeake Biological Laboratory (CBL) Graduate Education Committee, the University of Maryland Graduate School, the Marine Fisheries Section of the American Fisheries Society, the Maryland Department of Natural Resources, and the National Science Foundation under grant number OCE-1427019 for funding this work and/or my travel to several conferences.

This research would not have been possible without access to open-source software. Programs in this research included R (3.3.2), RStudio (1.0.136), with R packages automap, data.table, lavaan, maps, maptools, MARSS, RColorBrewer, rgdal, rgeos, rstan, semTools, sp, and tidyverse.

Thanks to my family - Caroline, Julia, Kay, and Walter Doering and Aras Zygas - for always supporting my choice to pursue a career in science.

My committee members, Drs. Lora Harris, Dong Liang, and Michael Wilberg provided me guidance throughout this project that has allowed me to grow as a scientist – I am deeply grateful. Thanks also to members of the Wilberg and Nesslage Labs during my time at CBL: Matthew Damiano, Jerelle Jesse, Emily Liljestrand, and Marvin “Trey” Mace III- I have learned so much from all of you. Finally, thanks to the CBL community for creating a welcoming environment - I feel honored to have been a part of it.

Table of Contents

List of Tables

List of Figures

Chapter 1: Patterns in oyster natural mortality in Chesapeake Bay, Maryland using a novel Bayesian estimator

Introduction

Natural mortality (i.e., all mortality due to non-fishing causes) is a key process in population dynamics. Stock assessment models typically require accurate estimates of natural mortality to obtain accurate estimates of abundance and fishery management reference points (Clark 1999, Deroba & Schueller 2013, Johnson et al. 2015). Despite this need, natural mortality is often difficult to estimate because natural mortality events are rarely observed for many organisms. A variety of approaches have been developed to infer a natural mortality rate in the absence of data, including methods that use growth parameters with environmental temperature (Pauly 1980) and longevity of the species (Hoenig 1983, Hewitt & Hoenig 2005). However, these techniques vary in their degree of reliability, and some perform poorly (Kenchington 2014). In addition, these methods only provide estimates of the average natural mortality rate over a relatively long period and thus cannot be used to understand the inter-annual variability of natural mortality.

Although observing, and hence estimating, natural mortality is difficult for most species, for many bivalves indirect observation of natural mortality frequently occurs. Bivalves often leave behind articulated valves (i.e., shells connected by the hinge ligament) when they die, providing evidence that natural mortality has occurred. Observations of articulated valves allow natural mortality to be estimated at much higher resolution than is possible for other organisms (e.g., Ford et al. 2006), although the time scale at which

natural mortality can be estimated depends in part on how long the articulated valves persist in the environment. For example, if the valves remain articulated for about one year, they can be used to estimate time-varying natural mortality on an annual scale. One caveat of using articulated valves to estimate natural mortality is that it only quantifies sources of mortality which leave behind articulated valves. For example, if the main source of natural mortality is a predator that crushes the shells of the bivalve during predation, this type of mortality will not leave behind articulated valves, and quantifying natural mortality using observations of articulated valves would be a poor choice for such a species. However, if a disease event is the primary cause of mortality, the valves of the bivalves that die often remain articulated, and disease mortality will be well represented using articulated valves to estimate the natural mortality rate.

Several estimators of natural mortality use counts of live bivalves and articulated valves (e.g., Dickie 1955, Caddy 1989, Ford et al. 2006, Walter et al. 2007, Vølstad et al. 2008), but these estimators have some shortcomings. First of all, some estimators are not formal statistical models, so uncertainty in the natural mortality rate is not quantified (e.g., Dickie 1955, Caddy 1989, Ford et al. 2006). Second, the assumptions of most estimators are restrictive and unrealistic for bivalves, and therefore are likely violated (e.g., Dickie 1955, Caddy 1989, Vølstad et al. 2008). For example, Dickie (1955) assumes a constant natural mortality rate such that the creation rate of articulated valves is equal to their disarticulation rate. Bivalves can experience large pulsed mortality events (e.g., Andrews & Wood 1967, Walter et al. 2007, Munroe et al. 2013), which would cause the natural mortality rate to change over time. In this case, the creation and disarticulation rates of

articulated valves are not in equilibrium, violating a key assumption of the estimator. Lastly, some estimators require additional data (e.g., Ford et al. 2006) or more frequent data collection than is typical (e.g., Ford et al. 2006, Walter et al. 2007). A statistical estimator for natural mortality that uses articulated valves with generalizable assumptions for bivalves and only requires annual (as opposed to more frequent) survey data has not been developed.

The eastern oyster *Crassostrea virginica* occurs in coastal ecosystems on the Atlantic Coast of North America from the Gulf of St. Lawrence, Canada to the Gulf of Mexico (Carriker & Gaffney 1996). Although eastern oysters were harvested commercially throughout their range historically, at present active oyster fisheries are fewer and much smaller because oysters are less abundant. Oysters are ecologically important in part because they build reefs (also known as bars) that provide habitat for other organisms, including fish, clams, amphipods, and polychaetes (Rodney & Paynter 2006), and because they are filter feeders that potentially exert top-down control on phytoplankton, sequestering nutrients and potentially reducing hypoxia in the Chesapeake Bay (Newell 1988, Newell et al. 2007). In particular, oyster bars may be important for nitrogen removal (Kellogg et al. 2013).

The eastern oyster in Chesapeake Bay, Maryland (upper Chesapeake Bay) supported the largest oyster fishery in the world at its peak in the 1880s, as the Maryland catch was double the total catch of all countries other than the US at this time (Kennedy & Breisch 1983). While harvest has declined since the 1880s peak, upper Chesapeake Bay still

supports an active commercial oyster fishery open from October to March. The harvest during the 2014-2015 season was 388,658 Maryland bushels in upper Chesapeake Bay, about 2% of historical peak harvest in Maryland (Tarnowski 2016). Despite harvest declines, the eastern oyster remains economically important in Maryland; for example, the Maryland harvest in 2014-2015 had a dockside value of $17.1 million USD (Tarnowski 2016).

The Maryland Department of Natural Resources (MDNR) conducts a fishery-independent survey for oysters each fall. One component of this monitoring is estimating the annual natural mortality rate (i.e., the proportion of oysters that die each year) using the "box count method" (a "box" is a set of articulated valves from an oyster; Ford et al. 2006). The box count mortality rate M_b is calculated by dividing the number of boxes in the sample, b, by the sum of the number of boxes and live oysters, l, in the same sample,

$$M_b = \frac{b}{b+l}. \quad (1)$$

Estimates of natural mortality rates for the Maryland portion of Chesapeake Bay are obtained using the box count method with samples from 43 fixed sites, which are then averaged to obtain the "observed" mortality index (Tarnowski 2017). While the box count method is a logical choice for these annual survey data because of its simple calculation and minimal data requirements (counts of live oysters and boxes from a single sample in a year is sufficient to calculate an estimate of natural mortality), it relies on strong assumptions to ensure unbiased estimates and is not a statistical estimator.

Violations of the assumptions of the box count method may lead to bias in the estimates of natural mortality obtained using the method. Some assumptions of the box count method include that 1) boxes persist in the environment for exactly one year, and 2) live oysters and boxes are equally collected and retained by the survey gear. These assumptions may be violated for oysters in the Maryland portion of Chesapeake Bay. Some boxes remain intact for less than one year, while others persist for longer than one year (Christmas et al. 1997, Ford et al. 2006). Additionally, the efficiency of dredge survey gear is lower for boxes than for live oysters (relative to divers; Powell et al. 2007; Marenghi et al. 2017). Efficiency is defined here as the number of live oysters or boxes that remain intact in a dredge sample relative to the number present per area swept (divers are assumed 100% efficient). Efficiency may be lower for boxes than for live oysters because boxes are more likely to be broken apart by the dredge, although other causes may also contribute.

The challenge of accurately estimating uncertainty is another limitation of the box count method because quantifying the uncertainty in the natural mortality rate is an important component of understanding natural mortality and its interannual variability. Because the box count method is not a statistical estimator, it can only provide point estimates of natural mortality. Design-based estimators (Thompson 2002) could be used with the ratio of boxes to live oysters to estimate uncertainty, but they are likely to overestimate the precision because observations of individual live oysters and boxes are treated as

independent. In addition, they also require applying the delta method because boxes are in the numerator and the denominator.

Despite their potential to result in biased estimates of natural mortality, the implications of using the box count method for a population that does not adequately meet its assumptions have not been investigated, nor have there been attempts to modify the method to correct for potential violations of the assumptions and to obtain more accurate estimates of uncertainty. Therefore, our objectives were twofold. First, we wanted to develop a new statistical method for estimating natural mortality using observations of live oysters and boxes that incorporates corrections for boxes persisting for longer than one year, accounts for unequal efficiencies between live oysters and boxes, and quantifies uncertainty. Then, we used this method to understand spatial and temporal patterns of oyster natural mortality in Maryland.

Methods

We developed a Bayesian model and fitted it to observations of adult (> 1 year old) live oysters and boxes from the MDNR fall dredge survey to estimate natural mortality rates for each year. Estimation of natural mortality was done spatially on the NOAA code level, where NOAA codes are the statistical catch reporting areas of the Maryland portion of Chesapeake Bay (Figure 1a). The Bayesian model differed from the box count method primarily because it allowed boxes to persist for longer than one year and estimated a rate at which boxes disarticulate, accounted for boxes disarticulating before the survey (i.e., some boxes that persisted for less than one year), and accounted for the differences in the ability of the survey dredge to collect and retain live oysters compared to its ability to

collect and retain boxes. We then investigated patterns in natural mortality among all NOAA codes by implementing dynamic factor analysis on time series of natural mortality by NOAA code as estimated from the Bayesian model.

Data

We used data on counts of adult live oysters and adult-sized boxes per half Maryland bushel (Maryland bushel ≈ 46 L) cultch in individual dredge tows from the fall dredge survey to inform parameter estimation in the model. The survey is described in Vølstad et al. (2008) and in greater detail in annual reports from MDNR (e.g., Tarnowski 2016). In short, the survey samples 66 fixed sites (i.e., bars) annually, but also includes additional non-random samples of interest to MDNR. A 32-inch oyster dredge was used to collect power-dredged oyster samples on more than 250 oyster bars each year. Distance towed was not standardized, but it was adjusted to obtain at least a half bushel of cultch, if possible, at each site. At most bars in a given year, only 1 tow was conducted (69.7% of bar and year combinations), but at least 2 replicate tows are completed at the 66 fixed sampling sites. Less than 1% of site and year combinations had more than 3 replicate tows. Adult oysters and adult-sized boxes were counted in a half bushel subsample of cultch from the dredge tow unless a half bushel sample from the dredge was not obtained. This rarely occurred (<1% of samples), so we normalized all data to per half Maryland bushel cultch. Spat (i.e., oysters < 1 year old) are also counted during the fall dredge survey but were not included in our analysis because spat boxes are rarely observed.

In the model, we used data from bars that were sampled at least once every year during 1990-2017 (i.e., the bar had a “complete time series”), because the model required

complete time series for each oyster bar. All NOAA codes with at least two bars with complete time series of dredge survey observations were included in the model to estimate natural mortality rates on the NOAA code level.

In the Maryland portion of Chesapeake Bay, 32 NOAA codes had sufficient data (i.e., a complete time series during 1990-2017 at ≥ 2 oyster bars) to estimate natural mortality using the Bayesian model. In total, data from 153 bars informed the model, where the median number of bars in a NOAA code with adequate data to include in the model was 5 (Table 1). In all, data from 6,722 dredge tows were used.

Model structure

The model was developed to estimate natural mortality rates by NOAA code from oyster bar-specific data. We used data on live oysters and boxes to estimate natural mortality rates, but also included a box dynamics model that addressed differences in efficiency in live oysters and boxes and the process of boxes disarticulating. By including the box dynamics, we were able to estimate a box decay rate of oysters in addition to the natural mortality rates.

Box dynamics model

The box dynamics model tracked a pool of boxes on each bar, including additions through natural mortality and losses through disarticulation. We calculated the mean number of boxes for a bar i in year y, $\beta_{i,y}$ as the sum of boxes from natural mortality that occurred in previous years that have not yet disarticulated and boxes from natural mortality that occurred in year y,

$$\beta_{i,y} = \beta_{i,y-1} e^{-d} + \frac{\delta_{i,y}}{R_q}, \quad (2)$$

where $\beta_{i,y-1}$ is the mean number of boxes from the previous year at the same bar, d is the instantaneous box disarticulation rate (i.e., the rate at which the hinge ligament connecting the two valves of a box fails; yr^{-1}), which was the same rate for all bars and years, $\delta_{i,y}$ is the number of oyster deaths at bar i in year y given the same efficiency as for live oysters, and R_q is the ratio of the efficiency of live oysters to the efficiency of boxes for all bars and years, which also includes a correction for boxes that disarticulate before the survey. Because of the time series structure of the box dynamics model, one additional year of data for boxes was required to estimate the number of boxes at the beginning of the time series. R_q converted $\delta_{i,y}$ from the efficiency of live oysters to that of boxes, which was necessary because the other term in the above equation assumed the efficiency of boxes. Thus, the model includes corrections for boxes persisting for longer than one year, unequal efficiencies for observing live oysters and boxes in the survey, and boxes disarticulating before the survey.

We parameterized the box dynamics portion of the model as a function of the natural mortality rate for each NOAA code. In the Maryland portion of Chesapeake Bay, the oyster fishery occurs in the fall and winter, while natural mortality mostly occurs in the summer (Ford et al. 2006, Albright et al. 2007). Because observations from the survey take place after natural mortality, we needed to parameterize the model to be in terms of the number of oysters alive after natural mortality and the natural mortality rate. The number of oysters that die from natural mortality, $\delta_{i,y}$, was calculated as the difference

between the number of live oysters before natural mortality and the number at the time of the survey,

$$\delta_{i,y} = \tau_{i,y} - \lambda_{i,y}, \tag{3}$$

where $\tau_{i,y}$ is the number of live oysters at bar i in year y after the fishing season ends and after growth has occurred but before natural mortality occurs, and $\lambda_{i,y}$ is the number of live oysters after natural mortality occurs at bar i in year y.

Because there was not a survey before natural mortality occurred, $\tau_{i,y}$ was not directly estimable using the fall dredge survey data, and a variable that could be estimated using the fall dredge survey data was needed. If natural mortality is the only source of mortality after the fishing season, $\lambda_{i,y}$ can be calculated as the product of $\tau_{i,y}$ and the annual survival rate over the period where natural mortality occurs,

$$\lambda_{i,y} = \tau_{i,y}(1 - M_{r,y}), \tag{4}$$

where $M_{r,y}$ is the annual natural mortality rate for oysters in NOAA code r and year y. Note that a common natural mortality rate was assumed for all bars within a NOAA code. The above equation can be solved for $\tau_{i,y}$,

$$\tau_{i,y} = \frac{\lambda_{i,y}}{1 - M_{r,y}}, \tag{5}$$

and then substituted into equation (3) to remove $\tau_{i,y}$ as a variable,

$$\delta_{i,y} = \frac{\lambda_{i,y}}{1 - M_{r,y}} - \lambda_{i,y}. \tag{6}$$

The number of oysters that die from natural mortality at bar i in year y, $\delta_{i,y}$, is now specified in terms of variables that are estimable using the fall dredge survey data ($\lambda_{i,y}$) or of interest ($M_{r,y}$). This equation was substituted for $\delta_{i,y}$ in equation (2) to get the complete box dynamics model as a function of the natural mortality rate,

$$\beta_{i,y} = \beta_{i,y-1} e^{-d} + \frac{\frac{\lambda_{i,y}}{1-M_{r,y}} - \lambda_{i,y}}{R_q}. \quad (7)$$

Parameter estimation

The joint posterior distribution of the parameters is given by

$$P(\theta \mid data) \propto Likelihood(\theta \mid data) \times priors(\theta), \quad (8)$$

where θ is the vector of estimated parameters and $priors(\theta)$ is the joint prior probability of the parameters.

The likelihood functions in the model described how well the model fits the observed number of live oysters or boxes. The model allowed multiple observations for a bar in a year. Observation n of the number of live adult oysters $l_{n,i,y}$ on bar i in year y followed a Poisson distribution with a mean parameter $\lambda_{i,y}$ for bar i in year y,

$$l_{n,i,y} \sim Pois(\lambda_{i,y}). \quad (9)$$

Likewise, observation n of the number of boxes $b_{n,i,y}$ on bar i in year y followed a Poisson distribution with a mean parameter $\beta_{i,y}$ specific for bar i and year y,

$$b_{n,i,y} \sim Pois(\beta_{i,y}). \quad (10)$$

Priors on the estimates of $\lambda_{i,y}$ were distributed normally on the $\log_e$ scale with a mean $log_e\Lambda_{r,y}$, specific for each NOAA code r and year y, and standard deviation σ, which is the same across NOAA codes and years,

$$log_e\lambda_{i,y} \sim N(log_e\Lambda_{r,y}, \sigma). \quad (11)$$

Similarly, $\log_e$ scale estimates of $\beta_{i,0}$ from different bars in the same NOAA code were assumed to be distributed normally with a mean parameter for year 0, $log_e B_{r,0}$, and standard deviation σ,

$$log_e\beta_{i,0} \sim N(log_e B_{r,0}, \sigma), \quad (12)$$

where σ is the same in equations (11) and (12). A uniform prior was placed on σ to restrict the parameter to a reasonable range between 0 and 3,

$$\sigma \sim uniform(0,3), \quad (13)$$

while normal priors were assumed for $log_e\Lambda_{r,y}$ and $log_e B_{r,0}$,

$$log_e\Lambda_{r,y} \sim N(\mu_\Lambda, \psi_\Lambda) \quad (14)$$

$$log_e B_{r,0} \sim N(\mu_B, \psi_B), \quad (15)$$

where μ_Λ and μ_B are means and ψ_Λ and ψ_B are standard deviations. The means μ_Λ and μ_B were estimated from the mean of all observed values of live oysters (for μ_Λ) and boxes (for μ_B) for all NOAA codes and years.[1] To ensure that these priors were relatively non-informative, ψ_Λ and ψ_B were both set at 5.

[1] Estimates of natural mortality and the box disarticulation rate were the same for a model that set the means at 0 instead of using the data.

For the box disarticulation rate, we used a normal prior with mean μ_d and standard deviation ϕ_d,

$$d \sim N(\mu_d, \phi_d), \tag{16}$$

where $\mu_d = 0.51$ and $\phi_d = 0.04$, based on results from box disarticulation studies (Christmas et al. 1997, Ford et al. 2006). The values for μ_d and ϕ_d were calculated using data on the mean time since death (d) for samples from each year, season, and habitat type in Christmas et al. (1997) and assuming exponential decay to convert mean time since death (d) to an instantaneous disarticulation rate (yr^{-1}). Instantaneous disarticulation rates (d^{-1}) were reported in Ford et al. (2006) and were converted to instantaneous disarticulation rates (yr^{-1}) for samples from each month and site. The mean and standard error of these estimates were used as estimates of μ_d and ϕ_d, respectively.

The annual natural mortality rate for each NOAA code and year, $M_{r,y}$, had priors that followed a diffuse beta distribution with α and β parameter values of 1,

$$M_{r,y} \sim Beta(1,1). \tag{17}$$

A beta distribution was chosen because annual natural mortality rates must be between 0 and 1.

The efficiency ratio R_q could not be estimated within the model because there was not enough information in the live oyster count and box count data to determine its value. Therefore, it was specified as a constant based on the averaged estimated efficiencies of live oysters and boxes from dredge efficiency studies (Powell et al. 2007, Marenghi et al.

2017) and on 20% of boxes disarticulating before the survey (Ford et al. 2006). The efficiency ratio was calculated for each life stage (juvenile, submarket, and market) and sampling location from data in the two studies by dividing efficiencies of live oysters by efficiencies of boxes and then averaging them to obtain an overall mean efficiency ratio that does not account for boxes disarticulating before the survey, 1.68. Ford et al. (2006) deployed boxes from recently sacrificed oysters in early July and checked them monthly for disarticulation; after about 100 days (in early October and 3 months after deployment), approximately 20% of the boxes had disarticulated, so we used this value as an approximate estimate of the percent of boxes from mortality that occurred in that year that would disarticulate before the fall dredge survey. To account for boxes disarticulating before the survey in the model, we divided the mean efficiency ratio (1.68) by the proportion of boxes remaining intact for the survey (0.8), and the resulting value was used for the efficiency ratio in the model,

$$R_q = 2.10. \tag{18}$$

The fundamental parameters (i.e., parameters estimated directly in the model) were $log_e\lambda_{i,y}$, $log_e\beta_{i,0}$, d, $M_{r,y}$, σ, $log_e\Lambda_{r,y}$, and $log_eB_{r,0}$.

Model implementation

The posterior distributions of the parameters were obtained using Stan through the R package RStan (Stan Development Team 2018). Stan uses Hamiltonian Monte Carlo with a No-U-Turn sampler (HMC/NUTS) to estimate marginal posterior distributions for all model parameters. Three independent chains were run with 2,000 burn-in iterations and 2,000 post-burn-in iterations per chain. The number of iterations was chosen such that

effective sample sizes were close to 1,000 for all model parameters. A model was considered to have converged if all three chains had similar posterior distributions for each parameter, as indicated by a Gelman and Rubin potential scale reduction statistic (Gelman & Rubin 1992) below 1.1 and if there were no divergent samples in the posterior. Divergent samples are a sampling issue unique to the algorithm used by Stan.

Broader regional grouping of model results

Throughout presentation of the results, we grouped results from NOAA codes into broader regions for easier comparison of spatial trends on a larger scale (Figure 1b). Note that these broader regions were not included in the model.

Comparison of model natural mortality with box count natural mortality

To compare the difference in the natural mortality estimated between the box count method and the Bayesian model, natural mortality rates on the NOAA code level were also calculated using the box count method and the same data used in the model. For each sample, an estimate of the natural mortality rate was calculated using equation (1), then these estimates were averaged by year and NOAA code to obtain an estimate of natural mortality from the box count method for a NOAA code in a year.

Dynamic factor analysis

We used dynamic factor analysis (DFA) to describe common trends in natural mortality among NOAA codes (e.g., Zuur et al. 2003, Peterson et al. 2017). Median estimates of natural mortality by year in each NOAA code from the Bayesian model were converted to instantaneous rates to better satisfy the normality assumption, and each time series was

standardized by subtracting the mean and dividing by the standard deviation of the time series. The mean and standard deviations were also examined for patterns.

We implemented DFA models in a similar manner to Zuur et al. (2003), Peterson et al. (2017), and Holmes et al. (2018). We used a covariance matrix with equal parameter value along the diagonal and zeros in the off-diagonals (i.e., equal variance and no covariance) for parsimony and because the standardized natural mortality estimates should have similar error variances given that they were estimated from the same types of data using the same model.

DFA models with one to four trends were compared using the corrected Akaike Information Criterion (AIC_c; Burnham & Anderson 2002). Models with AIC_c that were less than 5 units different from the lowest AIC_c were considered similar (Peterson et al. 2017), and the fits and observed values were examined. The most parsimonious model with the lowest AIC_c, given that the fits to the data were reasonable, was chosen as the "best" model. The "mean fit" diagnostic, the ratio of the sum of squared residuals to the sum of squared measured values (Zuur et al. 2003), was also used to identify poorly fitting models. As in Peterson et al. (2017), we considered values of mean fit approximately greater than 0.6 as indicative of poor model fit.

DFA models were implemented using the R package MARSS (Holmes et al. 2012), which uses a maximum likelihood approach to estimate parameter values. The models estimated common trends among NOAA codes, as well as loading on those trends. The

loadings on the DFA trends are a measure of how much a NOAA code influences each trend, and magnitudes of 0.2 or greater can be regarded as having a relatively strong influence (Zuur et al. 2003).

Results

Natural mortality from model and comparison with box count estimator

For all parameters, the Gelman and Rubin potential scale reduction statistic was below 1.1 and there were no divergent samples in any of the posteriors. The lowest effective sample size was 974 for the annual natural mortality estimate in NOAA code 99 (Wye River) in 2016. All other effective sample sizes were above 1,000, and most of the parameters had the maximum possible effective sample size of 6,000.

Throughout the results and discussion, we refer to estimates from the Bayesian model as "model natural mortality" and estimates from the box count method as "box count natural mortality." These estimates of natural mortality are reported on the annualized scale (proportion yr^{-1}) unless otherwise noted.

The estimated standard deviations (SDs) of the model natural mortality posterior distributions varied from 0.005 to 0.220, with an average of 0.040. Uncertainty was also consistent across years, with the average standard deviation by year varying from 0.027 in 2013 to 0.061 in 2003 and with a mean of 0.040. There was no clear relationship between the magnitude of the natural mortality rate and the amount of uncertainty associated with it.

The average (over years) of median instantaneous model natural mortality from the model by NOAA code during 1991-2017 varied from 0.12 to 0.47 (annualized: 0.12 to 0.37; Figure 2A). In general, average natural mortality was lower in both the northern part of the bay and farther upstream in the tributaries. Likewise, the standard deviations associated with the median instantaneous natural mortality were typically higher in parts of the bay where the average median instantaneous natural mortality was higher (Figure 2B). However, there were some exceptions. For example, the NOAA codes 053, 137, and 637 (located in the Choptank River region) were not among the highest average median natural mortalities relative to other NOAA codes, but they had the highest standard deviations (median instantaneous over years) of all modeled NOAA codes.

Model natural mortality was generally higher and more variable in the beginning of the time series (1991 to 2002) and lower and less variable at the end (2003 to 2017; Figures 3-9; Table 2). Despite similar temporal patterns, the year in which natural mortality first became lower and less variable differed among the regions of the bay.

In general, model natural mortality and box count natural mortality followed a similar pattern (Figures 3-9). During periods of low natural mortality over multiple years, the model estimates were either similar to or slightly higher than the box count estimates of natural mortality. However, there were two situations in which model natural mortality deviated from box count mortality in a consistent way. First, natural mortality from the model was often higher than the box count method estimates in years with a relatively high natural mortality event and in years with consistently low natural mortality (e.g.,

2002 in North Mid-Bay; Figure 3A). Secondly, in the two to three years following a relatively high natural mortality event, the model natural mortality was usually lower than the box count natural mortality (e.g., 2003-2005 in North Mid-Bay; Figure 3A).

In the sections below that refer to model natural mortality by region, averages (avgs) and standard deviations (SDs) unless otherwise noted were calculated by taking the average or the standard deviation of annual point estimates of the median model natural mortality from the years mentioned and all NOAA codes in the region (unless specific NOAA codes are mentioned).

Only one NOAA code (127, North Mid-Bay) in the Western Shore region had enough data to allow estimation of natural mortality using the model. Natural mortality was relatively low during 1991-1999 and 2003-2017 (avg = 0.10 yr^{-1}) and was elevated during 2000-2002 (avg = 0.43 yr^{-1}; Figure 3).

In the Chester River region, patterns of natural mortality for the two NOAA codes in the Chester River (131 and 231) were more similar to one another than to nearby Upper Bay (NOAA code 25) located in the Chesapeake Bay Mainstem (Figure 4). The Upper Bay had a unique pattern, with low natural mortality throughout the time series (time series avg = 0.11 yr^{-1}) except for two relatively high values in 1996 and 2011.The Chester River NOAA codes (131 and 231) had increased natural mortality during 2000-2002 (avg = 0.46 yr^{-1}), but the Lower Chester River (131) had additional high natural mortality events in 1992, 1996, and 2006 (avg = 0.42 yr^{-1}). The Mid Chester river (231) had smaller peaks

in natural mortality in 1996 and 2005 (avg = 0.26 yr^{-1}), as well as relatively high natural mortality in 2003.

Natural mortality was high during 2001-2002 and 2007 across all NOAA codes in the Eastern Bay region (Figure 5). The Wye and Miles Rivers (NOAA Codes 99 and 60) also had high natural mortality events in 1991 and 1992 (avg = 0.57 yr^{-1}) that did not occur in Eastern Bay. In addition, during 2011 – 2017 in all Eastern Bay region NOAA codes, there was a gradual increase in natural mortality, although natural mortality fluctuated interannually in the Miles River (NOAA Code 60).

Patterns of model natural mortality were more consistent among NOAA codes in the Choptank River region (Figure 6) than in the other regions. During 1991-2002, natural mortality was interannually variable in most NOAA codes with some years of high natural mortality. Lower and less variable natural mortality started in 2003-2004. All NOAA codes in the Choptank region had a consistent peak in natural mortality in 2002 (avg = 0.84 yr^{-1}), followed by (in most NOAA codes) lower natural mortality in 2003 (all NOAA code avg = 0.19 yr^{-1}).

Natural mortality for NOAA codes in the Patuxent River region had different patterns than the other regions (Figure 7). All Patuxent River NOAA codes had high natural mortality events, during 1991-1992 and 1999-2000 followed by a period of lower and less variable natural mortality that started around 2003. Patterns of natural mortality in the Upper and Lower Patuxent (NOAA codes 168 and 368) were similar, with high

natural mortality events in 2001 and 2002 that were not seen in Lower Bay West (NOAA code 229).

The Potomoc River region did not have as consistent of a pattern as some other regions (Figure 8). While most NOAA codes in the Potomac had several relatively high natural mortality events during 1999-2002, there were no other consistent patterns among NOAA codes. Some NOAA codes like the Lower Potomac River (177) had natural mortality that fluctuated throughout the time series, while other NOAA codes like the Mid Potomac River (277) had natural mortality that generally decreased over the time series (with the exception of high natural mortality events during 2000-2002).

In the NOAA codes of the Tangier Sound region, natural mortality was on average more than twice as high and more variable during 1991-2006 than during 2007-2017 (Figure 9). The patterns in natural mortality were not entirely consistent among all NOAA codes in the region, but all NOAA codes experienced relatively high natural mortality events in 1992 and 1999, and most NOAA codes had high natural mortality events in 1995. Many of the NOAA codes (six of eight) experienced low natural mortality in 1993, and all NOAA codes except Honga River (NOAA code 47) had low natural mortality in 2011.

Box disarticulation rate

One parameter was estimated for the box disarticulation rate for all NOAA codes and years. The instantaneous box disarticulation rate posterior was higher (avg = 1.11, corresponding with 67% of boxes disarticulating each year) than the prior that was

created from literature values (avg = 0.51 or 40% of boxes disarticulate each year; Figure 10).

Dynamic factor analysis

After standardizing the natural mortality time series, some common patterns among NOAA codes were visible (Figure 11). Most NOAA codes had substantial variability with several high peaks during 1991-2002, but few NOAA codes had high values after 2002. The DFA was able to describe the time series relatively well with two trends (Figure 12). The two-trend model had a lower AIC_c than the one, three, and four trend models, and it also had reasonable fitted values and a mean fit diagnostic (Table 3). Therefore, we selected the two-trend model.

The first DFA trend displayed a relatively stable pattern during 1991-1997 before a distinct increase in natural mortality during 1998-2002, followed by a decline in 2003-2005, and a relatively stable pattern during 2006-2017 (Figure 12). The second DFA trend indicated fluctuating natural mortality during 1991-2002 (with peaks in 1992, 1995, and 1999). After 2000, the trend was relatively low and consistent, except for a small peak in 2005.

Although there was variability among NOAA codes within regions, in general NOAA codes in the more northernly part of Chesapeake Bay had higher positive loadings on trend 1 than the southernly part, while the southern part had higher positive loadings on trend 2 (Figure 13). NOAA codes 025 and 377 (Upper Bay and Upper Potomac) did not

fall along the north-south gradient of loadings, as they had large negative loadings on trend 2 (-0.25 and -0.48, respectively).

Discussion

The Bayesian model and box count method had similar natural mortality patterns in most years, but the model often had slightly higher values than the box count method due to the opposing corrections included in the model. The amount of difference between the natural mortality rates estimated by the two methods depends on the values of the efficiency ratio (including the correction for boxes disarticulating before the survey) and the box disarticulation rate. If the dredge efficiency of live oysters is higher than that of boxes, the natural mortality rate estimated by the model is increased relative to assuming equal efficiency. Likewise, accounting for boxes decaying before the survey increases natural mortality estimates. In contrast, when boxes persist for longer than one year, the model will estimate lower natural mortality. For oysters in the Maryland portion of Chesapeake Bay, in most years the effect of correcting for dredge efficiency differences between live oysters and boxes and for boxes disarticulating before the survey was larger than the effect of correcting for boxes persisting for longer than one year. The opposing corrections that were not completely balanced resulted in model natural mortality rates that were slightly higher than box count natural mortality rates. For example, in a sensitivity run of the Bayesian model that did not incorporate a correction for boxes disarticulating before the survey, natural mortality estimates decreased by 17.8% on average across all years and NOAA codes.

However, in years following a high natural mortality event, model natural mortality estimates were substantially lower than box count estimates. The Bayesian model performs better than the box count method at estimating natural mortality rates, given that boxes are persisting for longer than one year as specified in the Bayesian model. This occurred because in the model, while the effect size of the corrections for difference in efficiency and for boxes disarticulating before the survey on the natural mortality rate remained the same as in all other years, the effect size of the correction for boxes persisting for longer than 1 year on the natural mortality rate increased. For all years, a constant proportion of boxes created during a natural mortality event remained intact through the next year (the constant proportion depends on the box disarticulation rate), but in years with a high natural mortality event, a higher number of boxes (per unit cultch) are created during a large natural mortality event, thus resulting in a higher number of boxes remaining the following year. Additionally, the effect of boxes from previous years on the natural mortality rate was often substantial in years after a high natural mortality event also because the number of oysters alive was reduced in next year. For example, in 2003 (the year after oyster bars in many NOAA codes experienced high mortality events), on average 68% of the boxes observed across bars were attributed to residual boxes (i.e., boxes from the previous year), while in 2016 (2015 was not a high mortality year), 34% of the observed boxes were treated as residual. In contrast, the box count method assumes that all boxes observed during the year following a high natural mortality event came from oysters that died in the same year (i.e., no boxes were treated as residual). Thus, the box count method estimated a higher rate of natural mortality in

the year following the natural mortality event compared to the model, which is an overestimate if boxes do persist longer than one year.

The patterns in natural mortality were consistent among most regions of the Maryland portion of Chesapeake Bay. In most NOAA codes, the trends and loadings from the dynamic factor analysis indicted that natural mortality increased substantially during 1999-2002 (trend 1), was more variable in the beginning of the time series (apparent in trend 2) and has consistently remained below average during 2006-2017 (trends 1 and 2). The trends from the dynamic factor analysis correspond qualitatively well with previous patterns of natural mortality in a Maryland-wide population dynamics model (Wilberg et al. 2011), as natural mortality was interannually variable before 2002, increased substantially during 1999-2002, and declined to low levels after 2002 in both the dynamic factor analysis trends and in the previous estimates.

Natural mortality from an oyster stock assessment for Maryland (Maryland Department of Natural Resources 2018) was estimated at the same spatial scale as the Bayesian model and thus could be directly compared to estimates from the Bayesian model. The natural mortality rates from both methods were correlated (Pearson correlation coefficient = 0.67), although natural mortality was higher in the stock assessment model than in the Bayesian model (i.e., 23% average natural mortality in the stock assessment model compared to 10% average in the Bayesian model). The difference among estimates is likely due to structural differences between the models. The stock assessment model used information about live oyster density changing over time (i.e., it followed density of

oysters by stage) and also estimated the difference in efficiency between live oysters and boxes as opposed to setting it as a constant as in the Bayesian model.

Different environmental conditions such as winter temperature, summer temperature, summer salinity, and disease levels could explain the spatial north-south gradient in the loadings on trends from the dynamic factor analysis. Most natural mortality on adult oysters in Maryland during 1991-2017 is likely caused by the diseases MSX and dermo (Ford & Tripp 1996), as there are few predators that can prey upon adult oysters in Maryland (White & Wilson 1996). However, levels of MSX and dermo in Maryland can vary spatially. For example, MSX is consistently found in the Tangier Sound region and spreads to other regions of the Maryland portion of Chesapeake Bay during years of low freshwater flow when salinity increases throughout the bay (Tarnowski 2017). Salinity and temperature can influence disease levels (Hewatt & Andrews 1956, Ford & Haskin 1982, Chu & La Peyre 1993, Bushek et al. 2012). Investigating the relationship between natural mortality, disease, and environmental conditions may allow for a better understanding of why natural mortality patterns differ regionally.

The Upper Bay and Upper Potomac (NOAA codes 25 and 377) had natural mortality patterns distinct from the patterns of other NOAA codes. This is likely because these regions are in the freshest parts of Chesapeake Bay where oysters persist and are subject to freshets that can cause localized oyster mortality events (MDNR 2001, Tarnowski 2012). Interestingly, freshets lower salinity and hence reduce MSX and dermo infection intensities (Ford 1985, La Peyre et al. 2003, 2009), so in most NOAA codes, natural

mortality due to disease (and hence natural mortality overall) should be lower when there are freshet-caused natural mortality events in the Upper Bay or Upper Potomac. This may explain why there were negative loadings in the Upper Bay and Upper Potomac for trend 2, but positive loadings in most other NOAA codes in Maryland.

Multiple hypotheses could explain the lower and less variable natural mortality since 2003. The relatively low natural mortality since 2003 could have been caused by environmental conditions unfavorable to disease during this period; for example, low salinity can inhibit the development of MSX and dermo (Haskin & Ford 1982, Albright et al. 2007). Since 2003, only 2 of 15 years have had lower than average streamflow into the Chesapeake Bay (a surrogate of bay-wide interannual variation in salinity), compared to 5 of 12 years during 1991-2002.[2] Alternatively, the relationships between environmental conditions, disease, and natural mortality rates may have changed over time. One possible mechanism is that oysters in the Maryland portion of Chesapeake Bay have acquired resistance to disease, defined as, "the relative ability of an organism to avoid infection or to withstand the effects of disease" (Ford & Tripp 1996). While evidence of resistance to MSX by oysters has been found in Delaware Bay (Haskin & Ford 1979, Ford & Bushek 2012, Bushek & Ford 2016) and in the Virginia portion of Chesapeake Bay (Carnegie & Burreson 2011), it has not been documented in the Maryland portion of Chesapeake Bay. Evidence of dermo resistance has been found in oysters from Tangier Sound (Encomio et al. 2005), but not in oysters from the Choptank (Encomio et al. 2005), near Annapolis, Maryland (Brown et al. 2005b), or in Delaware

[2] Data available at https://md.water.usgs.gov/waterdata/chesinflow/annualized/data.

Bay (Bushek & Ford 2016). Investigating the relationship between environmental conditions, disease, and natural mortality before and since 2002 may illuminate if indeed favorable environmental conditions have kept disease levels low in recent years or if there has been a change in how oysters respond to either disease.

The Bayesian model required information on relative efficiency and box disarticulation rates to correct for these effects, which may differ depending on the survey gear (Chai et al. 1992), habitat characteristics (Powell et al. 2007), or oyster density (Morson et al. 2018). Because survey efficiency experiments on both boxes and live oysters have not been published for Maryland, we only used one estimate of relative efficiency for all NOAA codes and years derived from survey efficiency experiments conducted in Delaware Bay. Further investigation into the factors affecting relative efficiency may allow for better understanding of which factors influence relative efficiency of live oysters and boxes, which would allow these factors to inform different values of relative efficiency by NOAA code and year. Without additional efficiency data, it is unlikely that relative efficiency could be estimated in the model.

A key assumption of methods using counts of live oysters and boxes to estimate natural mortality is that the main sources of natural mortality leave behind boxes. Any natural mortality that does not will not be quantified, although the model could be modified to account for a proportion of mortality that does not leave behind a box. For adult oysters in Maryland, assuming all natural mortality leaves behind a box is reasonable, as the largest sources of natural mortality, MSX and dermo diseases and freshets, result in

boxes. Predation caused by organisms that crush shells of their prey would not be captured in the box count method nor model, but few predators can crush the shells of adult oysters (White & Wilson 1996). Thus, predation not resulting in a box is likely negligible for oysters in Maryland.

The posterior of the box decay rate was higher than its prior, suggesting that a higher proportion of boxes decay in a year than described by the prior. Our prior was based on field experiments in which oysters were sacrificed, and the resulting boxes were attached to trays or racks deployed on or near oyster bars and periodically monitored for disarticulation (Christmas et al. 1997, Ford et al. 2006). A faster disarticulation rate in the model of wild oysters on natural bars than these experiments is expected for two reasons. First, boxes in experiments are not exposed to wave action and other disturbance processes like they would be on a natural oyster bar. For example, Christmas et al. (1997) attached oysters to treys that were covered with lids, specifically because "wave action and storm events resulted in the periodic loss of oysters from uncovered trays." Second, oyster fishing during the winter likely breaks up some boxes on bars, which would result in a higher estimated disarticulation rate like we found in the model.

Our Bayesian natural mortality model could be applied to other bivalve populations or other species that leave long term evidence of natural mortality. The observations of live and dead individuals must occur in the same gear, however, so our approach would likely be limited to molluscs or other sessile or slow-moving species. Our approach has the potential to reduce bias in estimated natural mortality rates when assumptions of other

methods are violated. However, some modifications to the model would be necessary. The priors in our current version were tailored for oysters in the Maryland portion of Chesapeake Bay and would need to be modified for application to another species or oysters in a different region. In particular, the disarticulation rate of boxes likely differs among bivalve species and among locations (location: Christmas et al. 1997; Ford et al. 2006). In addition, fishing and natural mortality happen at different times for oysters in the Maryland portion of Chesapeake Bay, and this is a key assumption of the model. The model would need additional modifications and data for populations where fishing and natural mortality occur simultaneously.

This model and analysis illuminated the implications of assumptions of the box count method, corrected for these assumptions, and provided natural mortality estimates in Maryland at a finer spatial scale than previously available without using a full population dynamics model and additional data sources. In addition, the model we developed, albeit with some modifications, could be generalized to other bivalve populations or other species that leave long-term evidence of natural mortality.

Tables

Table 1. Number of bars with complete time series by region (names in bold between lines) and NOAA code. A bar with a complete time series is one that was sampled at least once every year during 1990-2017. NA indicates that natural mortality in the NOAA code was not modeled because of inadequate data.

NOAA Code	NOAA Code Name	Number of Bars
Western Shore		
127	North Mid-Bay	5
55	Magothy River	NA
82	Severn River	NA
88	South River	NA
94	West & Rhode Rivers	NA
Chester River		
25	Upper Bay	11
131	Lower Chester River	2
231	Mid Chester River	6
331	Upper Chester River	NA
Eastern		
39	Eastern Bay	6
99	Wye River	3
60	Miles River	4
Choptank River		
27	South Mid-Bay	6
437	Harris Creek	2
537	Broad Creek	2
637	Tred Avon River	4
137	Lower Choptank River	4
237	Mid Choptank River	6
337	Upper Choptank River	6
53	Little Choptank River	6
Patuxent River		
229	Lower Bay West	3
168	Lower Patuxent River	6
268	Mid Patuxent River	NA
368	Upper Patuxent River	5
Potomac River		
177	Lower Potomac River	4
86	Smith Creek	NA
78	St. Mary's River	5
277	Mid Potomac River	5
174	Breton & St. Clements	2
274	Wicomico River (West)	5
377	Upper Potomac River	4
Tangier Sound		
129	Lower Bay East	NA
47	Honga River	5
43	Fishing Bay	5
62	Nanticoke River	6
292	Tangier Sound North	3
96	Wicomico River (East)	3
98	Monie Bay	NA
192	Tangier Sound South	9
57	Manokin River	5
5	Big Annemessex River	NA
72	Pocomoke Sound	5

Table 2. Median natural mortality rate (fraction yr^{-1}) from the Bayesian model by region and NOAA Code during 1991-2017 and the time series mean. Names in bold between lines indicate the region in which the NOAA codes were grouped.

NOAA Code	1991	1992	1993	1994	1995	1996	1997	1998	1999	2000	2001	2002	2003	2004	2005	2006
Western Shore																
127	0.116	0.027	0.135	0.173	0.123	0.211	0.101	0.124	0.190	0.314	0.336	0.635	0.144	0.028	0.015	0.166
55	NA	NA	NA	NA	NA	NA	NA	NA	NA	NA	NA	NA	NA	NA	NA	NA
82	NA	NA	NA	NA	NA	NA	NA	NA	NA	NA	NA	NA	NA	NA	NA	NA
88	NA	NA	NA	NA	NA	NA	NA	NA	NA	NA	NA	NA	NA	NA	NA	NA
94	NA	NA	NA	NA	NA	NA	NA	NA	NA	NA	NA	NA	NA	NA	NA	NA
Chester River																
25	0.065	0.085	0.058	0.222	0.011	0.382	0.009	0.101	0.072	0.177	0.068	0.217	0.059	0.079	0.007	0.075
131	0.172	0.405	0.064	0.193	0.083	0.434	0.046	0.092	0.168	0.357	0.420	0.570	0.245	0.040	0.011	0.413
231	0.053	0.090	0.052	0.181	0.097	0.260	0.071	0.075	0.101	0.295	0.520	0.590	0.332	0.040	0.267	0.059
331	NA	NA	NA	NA	NA	NA	NA	NA	NA	NA	NA	NA	NA	NA	NA	NA
Eastern Bay																
39	0.222	0.412	0.337	0.217	0.365	0.199	0.129	0.133	0.315	0.342	0.496	0.582	0.121	0.011	0.064	0.530
99	0.653	0.539	0.095	0.233	0.366	0.074	0.110	0.133	0.213	0.450	0.498	0.622	0.543	0.036	0.040	0.089
60	0.541	0.558	0.296	0.204	0.413	0.244	0.023	0.186	0.219	0.361	0.505	0.650	0.393	0.034	0.105	0.434
Choptank River																
27	0.126	0.657	0.385	0.297	0.544	0.273	0.223	0.345	0.434	0.569	0.390	0.801	0.013	0.014	0.027	0.220
437	0.509	0.283	0.385	0.044	0.305	0.116	0.113	0.086	0.339	0.102	0.287	0.896	0.098	0.025	0.014	0.039
537	0.682	0.484	0.145	0.018	0.383	0.118	0.094	0.175	0.551	0.074	0.429	0.844	0.085	0.008	0.004	0.019
637	0.798	0.531	0.364	0.061	0.352	0.127	0.092	0.145	0.508	0.494	0.301	0.904	0.474	0.196	0.048	0.050
137	0.432	0.573	0.261	0.023	0.312	0.113	0.067	0.128	0.414	0.435	0.583	0.943	0.078	0.024	0.009	0.012
237	0.432	0.682	0.551	0.046	0.257	0.279	0.064	0.041	0.221	0.503	0.370	0.851	0.218	0.103	0.052	0.138
337	0.093	0.319	0.317	0.144	0.127	0.161	0.021	0.132	0.100	0.252	0.283	0.552	0.522	0.150	0.054	0.074
53	0.583	0.561	0.263	0.006	0.251	0.055	0.116	0.189	0.407	0.389	0.633	0.961	0.030	0.007	0.008	0.124
Patuxent River																
229	0.720	0.887	0.031	0.025	0.271	0.384	0.196	0.327	0.533	0.679	0.153	0.288	0.104	0.013	0.175	0.217
168	0.662	0.865	0.212	0.214	0.285	0.404	0.117	0.370	0.748	0.590	0.629	0.644	0.013	0.058	0.281	0.452
268	NA	NA	NA	NA	NA	NA	NA	NA	NA	NA	NA	NA	NA	NA	NA	NA
368	0.558	0.702	0.046	0.060	0.138	0.048	0.077	0.072	0.516	0.600	0.583	0.627	0.020	0.085	0.148	0.198

Table 2, continued.

NOAA Code	1991	1992	1993	1994	1995	1996	1997	1998	1999	2000	2001	2002	2003	2004	2005	2006
Potomac River																
177	0.507	0.692	0.148	0.110	0.636	0.156	0.171	0.303	0.881	0.616	0.121	0.614	0.153	0.302	0.391	0.375
86	NA	NA	NA	NA	NA	NA	NA	NA	NA	NA	NA	NA	NA	NA	NA	NA
78	0.234	0.360	0.171	0.152	0.202	0.207	0.164	0.162	0.466	0.679	0.399	0.814	0.045	0.486	0.561	0.013
277	0.496	0.216	0.215	0.114	0.201	0.140	0.050	0.262	0.298	0.605	0.662	0.744	0.105	0.306	0.256	0.185
174	0.685	0.238	0.054	0.224	0.503	0.105	0.256	0.276	0.531	0.761	0.674	0.742	0.189	0.310	0.333	0.113
274	0.260	0.190	0.038	0.053	0.297	0.250	0.038	0.062	0.370	0.375	0.448	0.596	0.131	0.123	0.055	0.221
377	0.022	0.083	0.451	0.479	0.011	0.168	0.097	0.260	0.024	0.062	0.167	0.525	0.416	0.337	0.026	0.021
Tangier Sound																
129	NA	NA	NA	NA	NA	NA	NA	NA	NA	NA	NA	NA	NA	NA	NA	NA
47	0.583	0.778	0.035	0.104	0.578	0.177	0.228	0.533	0.653	0.236	0.442	0.327	0.091	0.345	0.514	0.096
43	0.378	0.683	0.349	0.055	0.598	0.700	0.482	0.085	0.695	0.750	0.454	0.710	0.349	0.406	0.337	0.249
62	0.123	0.559	0.075	0.224	0.160	0.141	0.174	0.059	0.661	0.098	0.325	0.642	0.304	0.213	0.100	0.258
292	0.399	0.802	0.090	0.150	0.796	0.583	0.165	0.222	0.716	0.306	0.252	0.517	0.264	0.479	0.523	0.239
96	0.040	0.733	0.357	0.237	0.358	0.232	0.328	0.172	0.796	0.566	0.361	0.531	0.182	0.312	0.069	0.151
98	NA	NA	NA	NA	NA	NA	NA	NA	NA	NA	NA	NA	NA	NA	NA	NA
192	0.520	0.763	0.175	0.256	0.766	0.304	0.172	0.355	0.589	0.287	0.395	0.479	0.316	0.368	0.324	0.192
57	0.527	0.683	0.052	0.271	0.821	0.261	0.154	0.215	0.665	0.266	0.274	0.328	0.102	0.331	0.748	0.049
5	NA	NA	NA	NA	NA	NA	NA	NA	NA	NA	NA	NA	NA	NA	NA	NA
72	0.579	0.572	0.059	0.278	0.856	0.216	0.424	0.299	0.539	0.255	0.457	0.437	0.093	0.185	0.295	0.090

Table 2, continued.

NOAA Code	2007	2008	2009	2010	2011	2012	2013	2014	2015	2016	2017	Mean
Western Shore												
127	0.041	0.172	0.109	0.060	0.027	0.063	0.049	0.032	0.032	0.063	0.119	0.133
55	NA	NA	NA	NA	NA	NA	NA	NA	NA	NA	NA	NA
82	NA	NA	NA	NA	NA	NA	NA	NA	NA	NA	NA	NA
88	NA	NA	NA	NA	NA	NA	NA	NA	NA	NA	NA	NA
94	NA	NA	NA	NA	NA	NA	NA	NA	NA	NA	NA	NA
Chester River												
25	0.063	0.091	0.042	0.164	0.563	0.017	0.108	0.010	0.096	0.014	0.007	0.106
131	0.271	0.328	0.274	0.089	0.135	0.088	0.112	0.076	0.034	0.094	0.062	0.196
231	0.135	0.072	0.085	0.144	0.086	0.071	0.052	0.173	0.037	0.164	0.033	0.153
331	NA	NA	NA	NA	NA	NA	NA	NA	NA	NA	NA	NA
Eastern Bay												
39	0.609	0.220	0.239	0.110	0.048	0.026	0.069	0.112	0.066	0.201	0.246	0.238
99	0.310	0.307	0.257	0.341	0.028	0.035	0.023	0.079	0.113	0.227	0.333	0.250
60	0.622	0.396	0.299	0.086	0.055	0.082	0.022	0.136	0.038	0.208	0.118	0.268
Choptank River												
27	0.020	0.258	0.201	0.162	0.053	0.019	0.048	0.084	0.241	0.273	0.300	0.258
437	0.181	0.108	0.060	0.067	0.030	0.003	0.099	0.012	0.080	0.227	0.059	0.169
537	0.075	0.149	0.050	0.064	0.032	0.024	0.074	0.078	0.182	0.111	0.035	0.185
637	0.116	0.057	0.184	0.095	0.026	0.153	0.128	0.107	0.185	0.254	0.176	0.256
137	0.100	0.125	0.065	0.072	0.051	0.052	0.086	0.084	0.196	0.315	0.249	0.215
237	0.103	0.044	0.030	0.109	0.084	0.068	0.128	0.172	0.063	0.319	0.094	0.223
337	0.052	0.068	0.080	0.077	0.072	0.050	0.146	0.022	0.072	0.150	0.179	0.158
53	0.213	0.182	0.277	0.287	0.021	0.176	0.179	0.151	0.187	0.413	0.193	0.254
Patuxent River												
229	0.422	0.077	0.212	0.112	0.137	0.018	0.125	0.063	0.208	0.304	0.067	0.250
168	0.265	0.100	0.226	0.252	0.039	0.195	0.165	0.096	0.275	0.341	0.077	0.318
268	NA	NA	NA	NA	NA	NA	NA	NA	NA	NA	NA	NA
368	0.036	0.214	0.142	0.195	0.021	0.111	0.110	0.078	0.132	0.215	0.051	0.214

Table 2, continued.

NOAA Code	2007	2008	2009	2010	2011	2012	2013	2014	2015	2016	2017	Mean
Potomac River												
177	0.159	0.318	0.455	0.258	0.110	0.104	0.223	0.117	0.189	0.563	0.033	0.322
86	NA	NA	NA	NA	NA	NA	NA	NA	NA	NA	NA	NA
78	0.029	0.167	0.280	0.208	0.050	0.123	0.050	0.168	0.214	0.425	0.105	0.257
277	0.127	0.088	0.103	0.210	0.053	0.127	0.116	0.108	0.163	0.054	0.044	0.224
174	0.105	0.072	0.060	0.081	0.378	0.301	0.052	0.172	0.147	0.099	0.084	0.279
274	0.402	0.230	0.055	0.231	0.082	0.112	0.150	0.032	0.062	0.096	0.012	0.184
377	0.055	0.139	0.059	0.170	0.212	0.124	0.204	0.047	0.058	0.054	0.094	0.162
Tangier Sound												
129	NA	NA	NA	NA	NA	NA	NA	NA	NA	NA	NA	NA
47	0.038	0.098	0.186	0.163	0.140	0.187	0.217	0.159	0.229	0.152	0.229	0.278
43	0.023	0.076	0.081	0.082	0.044	0.132	0.158	0.217	0.179	0.228	0.011	0.315
62	0.084	0.127	0.075	0.078	0.102	0.170	0.051	0.113	0.075	0.167	0.082	0.194
292	0.178	0.039	0.262	0.288	0.152	0.158	0.181	0.217	0.254	0.214	0.020	0.314
96	0.388	0.146	0.052	0.135	0.058	0.069	0.142	0.180	0.344	0.462	0.200	0.282
98	NA	NA	NA	NA	NA	NA	NA	NA	NA	NA	NA	NA
192	0.114	0.203	0.258	0.307	0.091	0.156	0.160	0.355	0.246	0.059	0.113	0.308
57	0.054	0.198	0.153	0.244	0.035	0.210	0.172	0.166	0.159	0.162	0.140	0.275
5	NA	NA	NA	NA	NA	NA	NA	NA	NA	NA	NA	NA
72	0.021	0.288	0.170	0.127	0.034	0.146	0.145	0.188	0.182	0.091	0.182	0.267

Table 3. Corrected Akaike's Information Criterion (AICc) and mean fit comparisons of dynamic factor analysis with different numbers of trends. The differences in the AIC_c values (ΔAICc) were calculated as the difference in AIC_c between a given model and the one with the lowest AIC_c. The mean fit comparison is calculated as in Zuur et al. (2003) and Peterson et al. (2017).

Number of Trends	ΔAICc	Mean Fit
1	163.0	0.49
2	0.0	0.32
3	2.4	0.27
4	18.3	0.23

Figures

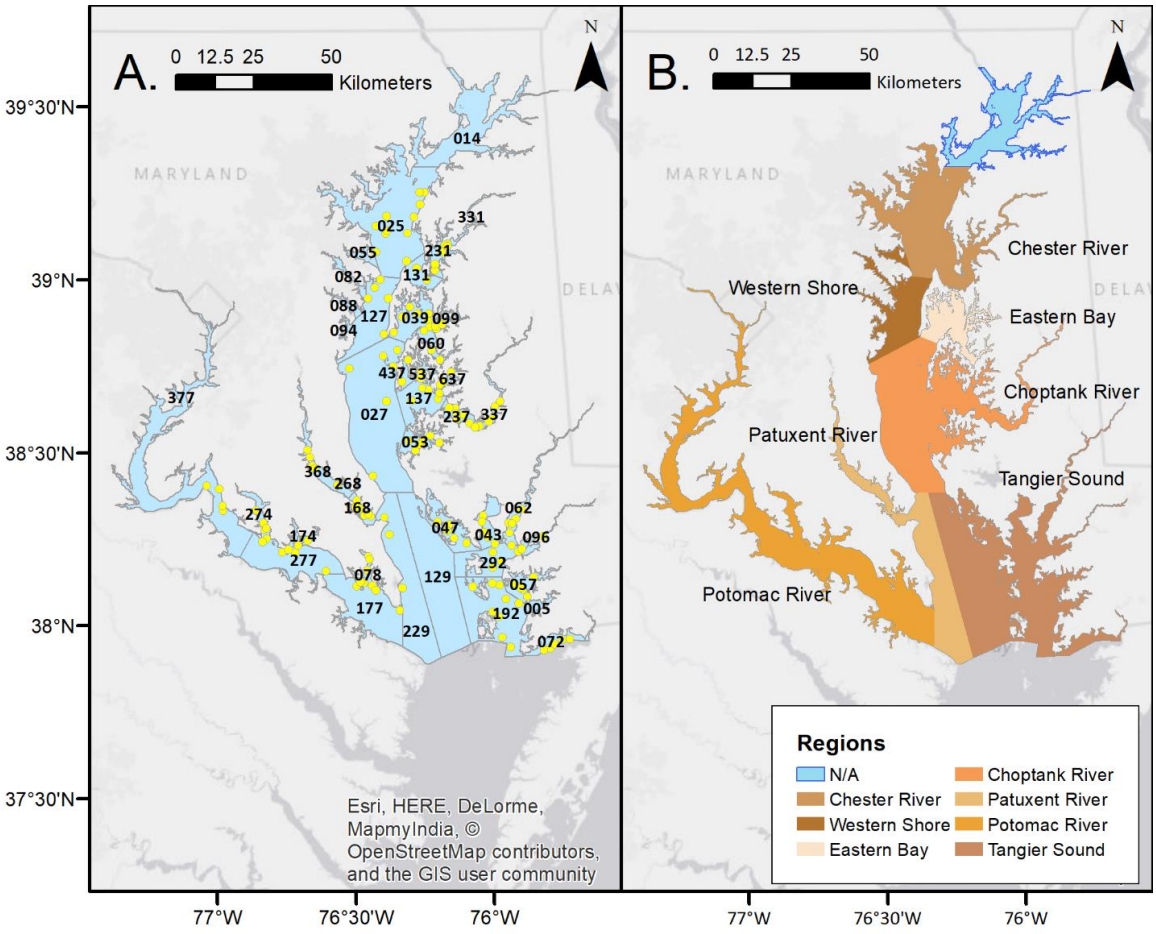

Figure 1. Maps of the Maryland Portion of Chesapeake Bay denoting A) NOAA codes (numbers in black text; see Table 1 for NOAA code names) and B) regions. Note that NOAA Code 14 was not included in a region because it likely has no oyster bars and is not sampled during the fall dredge survey. Yellow points mark the approximate locations of bars that were included in the model.

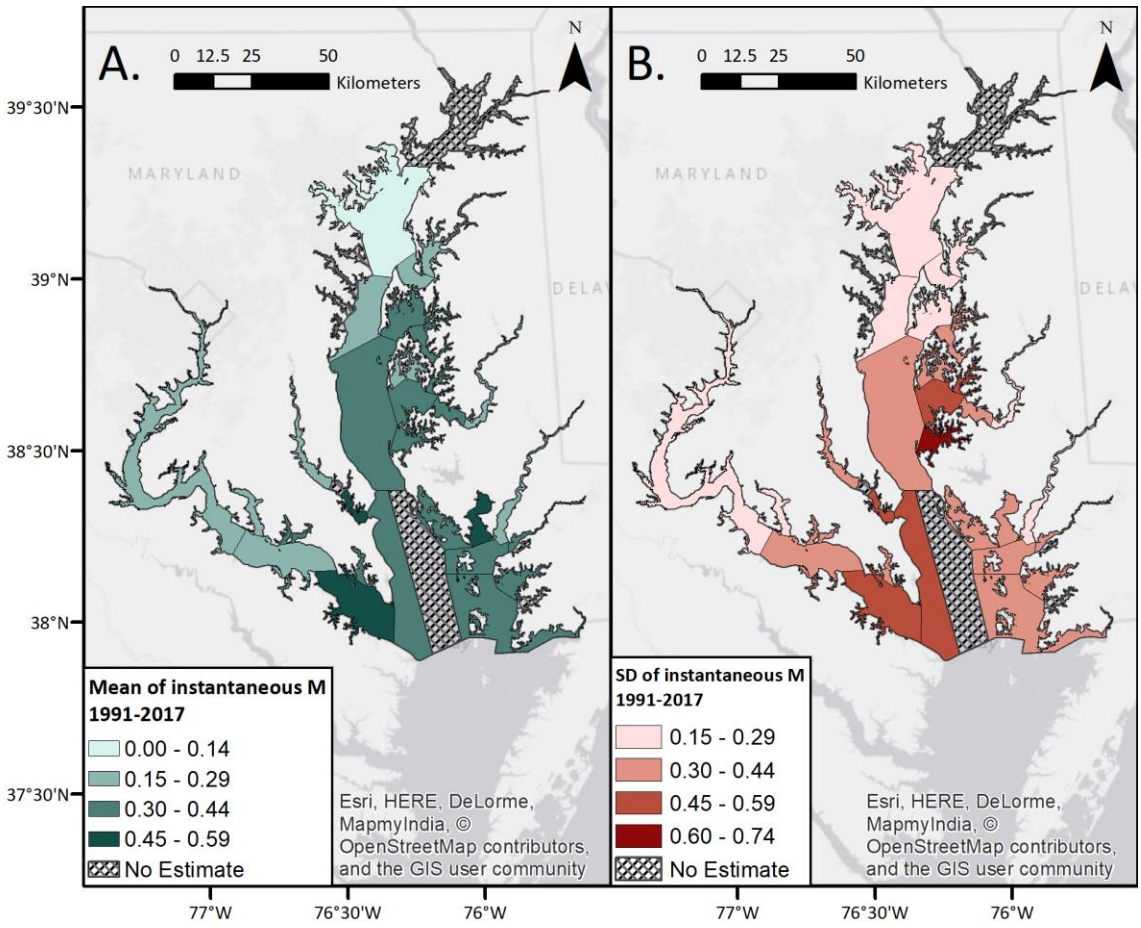

Figure 2. A) Mean and B) standard deviation (SD) of the times series of model instantaneous natural mortality (M; yr^{-1}) medians by NOAA code. Darker colors indicate a higher mean or standard deviation over the time series, and crosshatching indicates NOAA codes that were not modeled due to insufficient data.

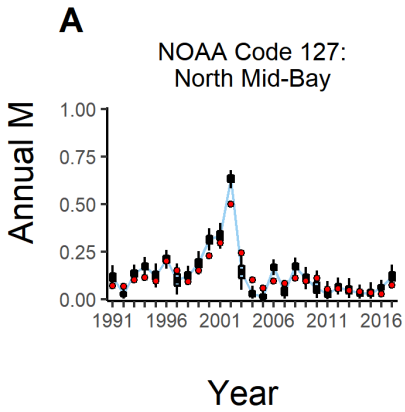

Figure 3. Natural mortality rate estimates (M; proportion yr^{-1}) for adult oysters from the model (boxplots) and the box count method (points) for NOAA codes of the Western Shore region. For the boxplot, the box represents the interquartile range, the line the median, and the whiskers 95% credibility intervals. The solid blue line connects the median values of the boxplots. The year labels correspond with the calendar year of when the natural mortality occurred.

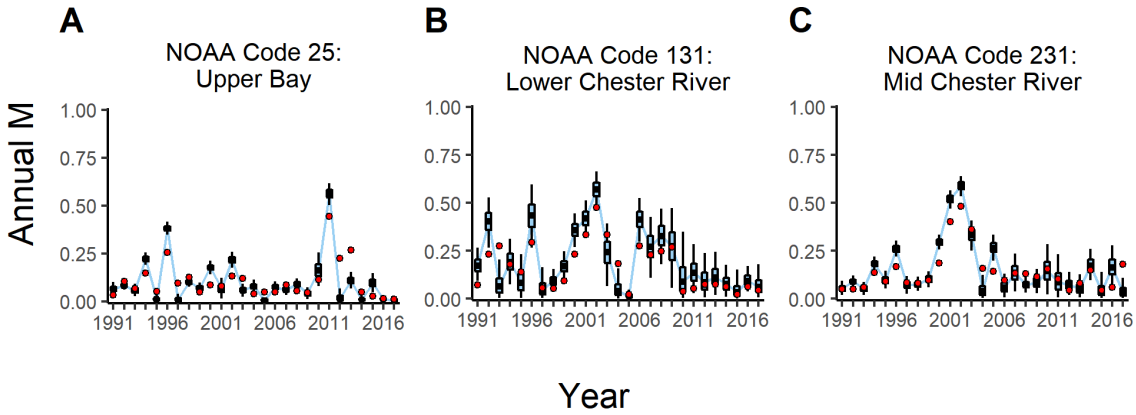

Figure 4. Natural mortality rate estimates (M; proportion yr^{-1}) for the Chester River region. Symbol definitions are the same as Figure 3.

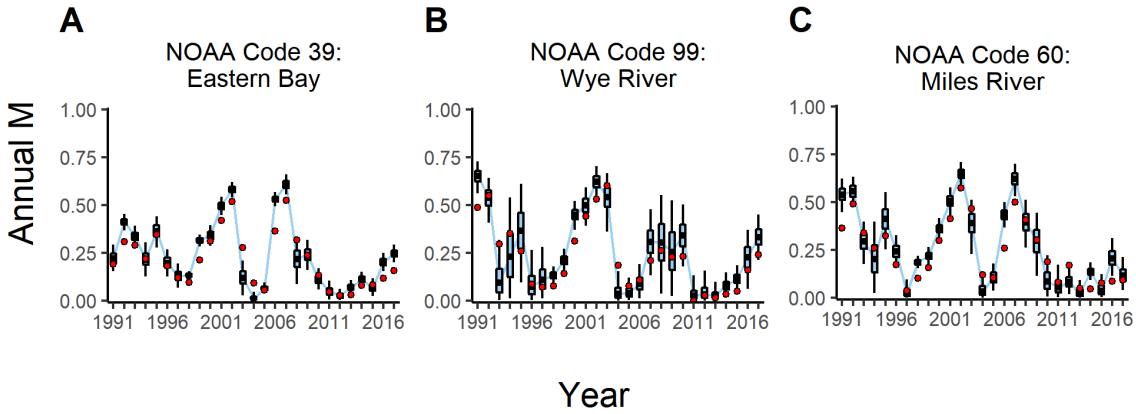

Figure 5. Natural mortality rate estimates (M; proportion yr^{-1}) for the Eastern Bay region. Symbol definitions are the same as Figure 3.

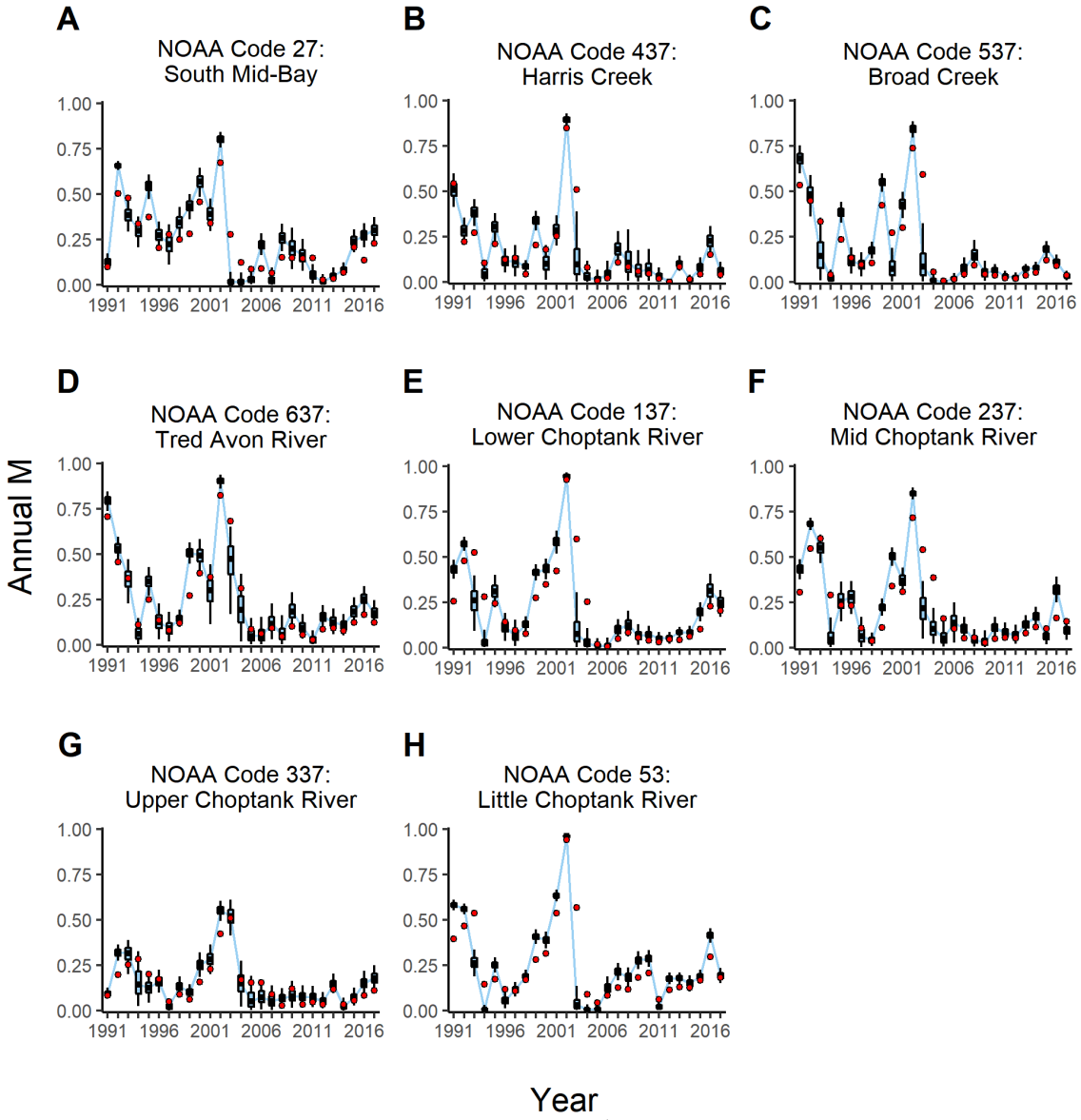

Figure 6. Natural mortality rate estimates (M; proportion yr^{-1}) for the Choptank River region. Symbol definitions are the same as Figure 3.

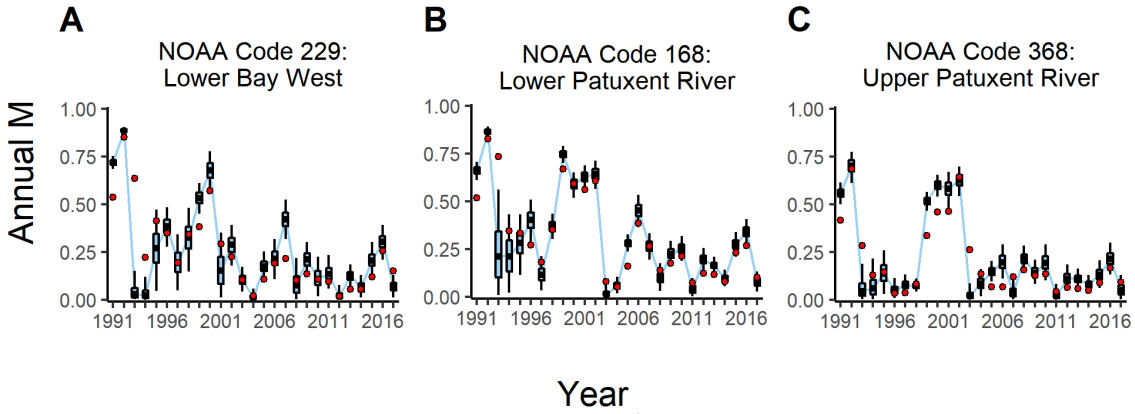

Figure 7. Natural mortality rate estimates (M; proportion yr^{-1}) for the Patuxent River region. Symbol definitions are the same as Figure 3.

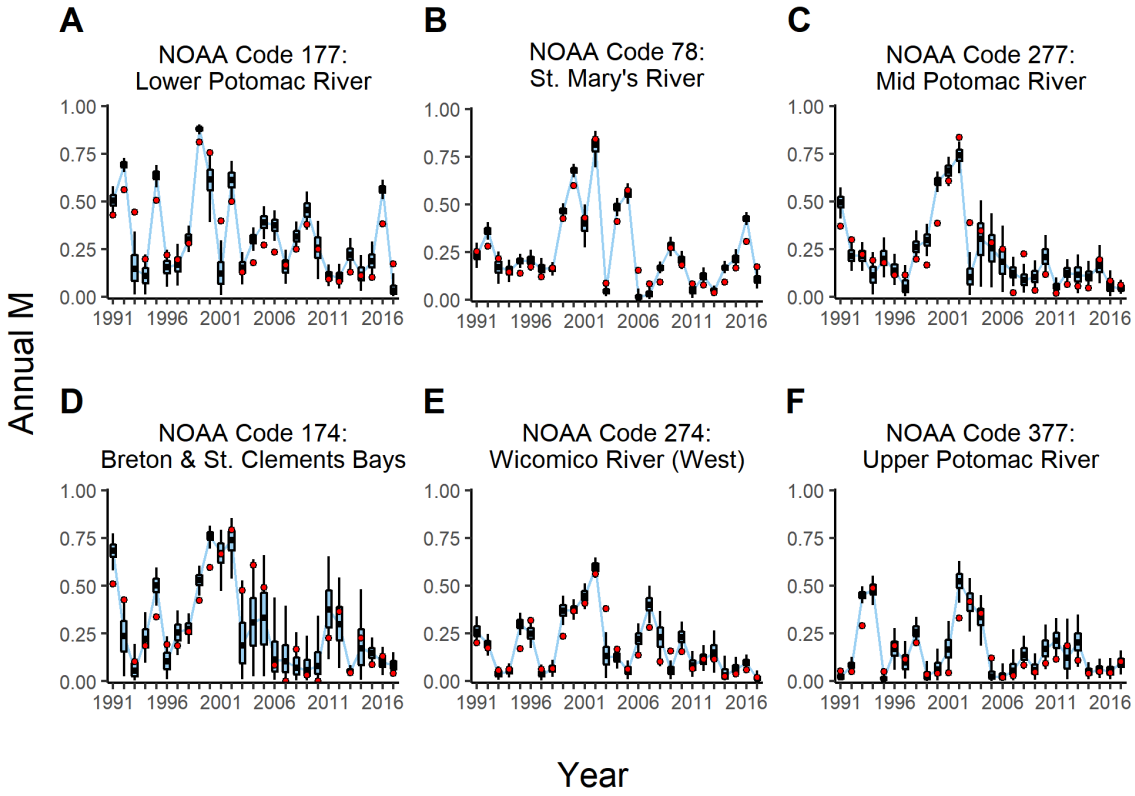

Figure 8. Natural mortality rate estimates (M; proportion yr^{-1}) for the Potomac River region. Symbol definitions are the same as Figure 3.

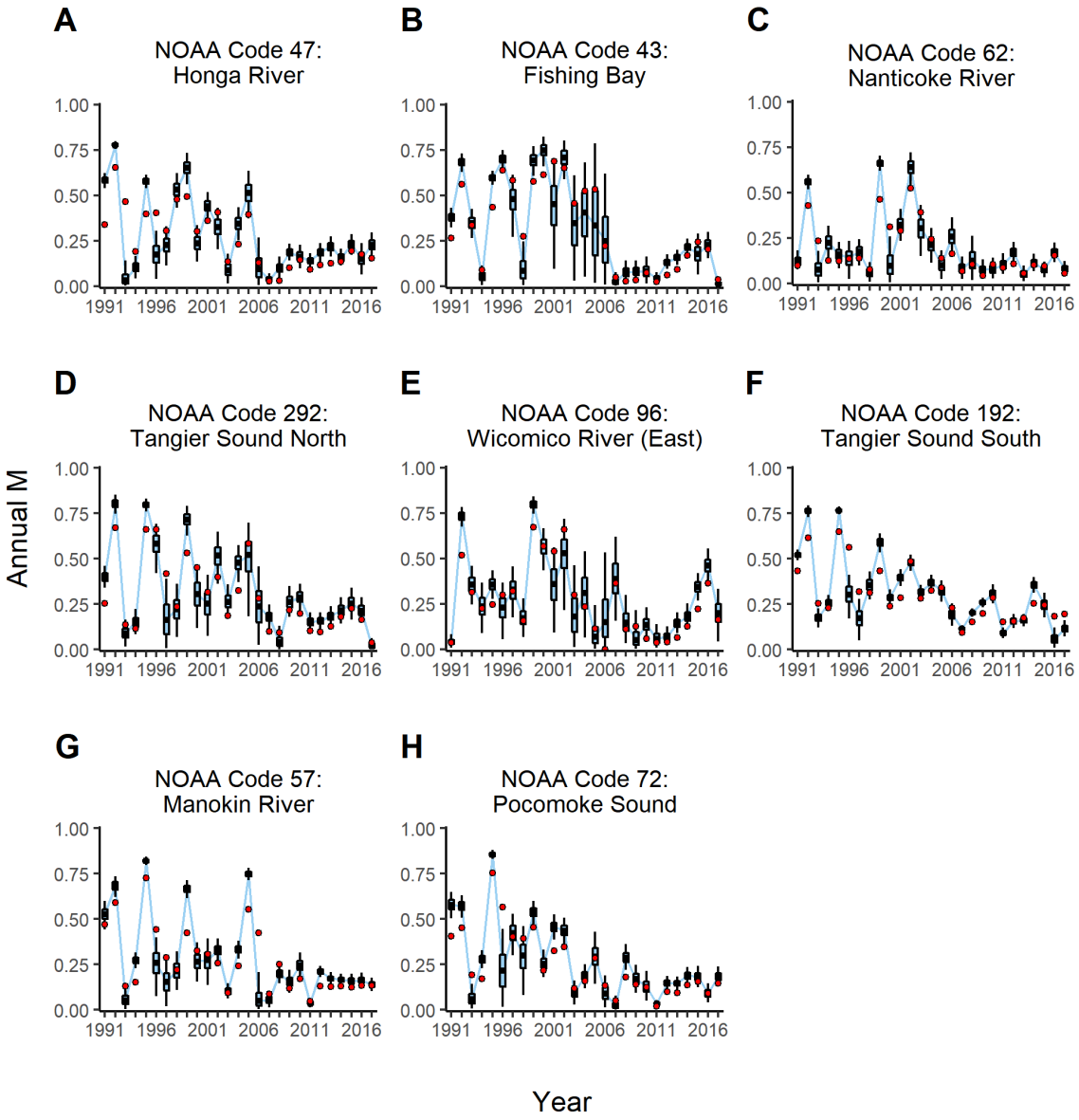

Figure 9. Natural mortality rate estimates (M; proportion yr^{-1}) for the Tangier Sound region. Symbol definitions are the same as Figure 3.

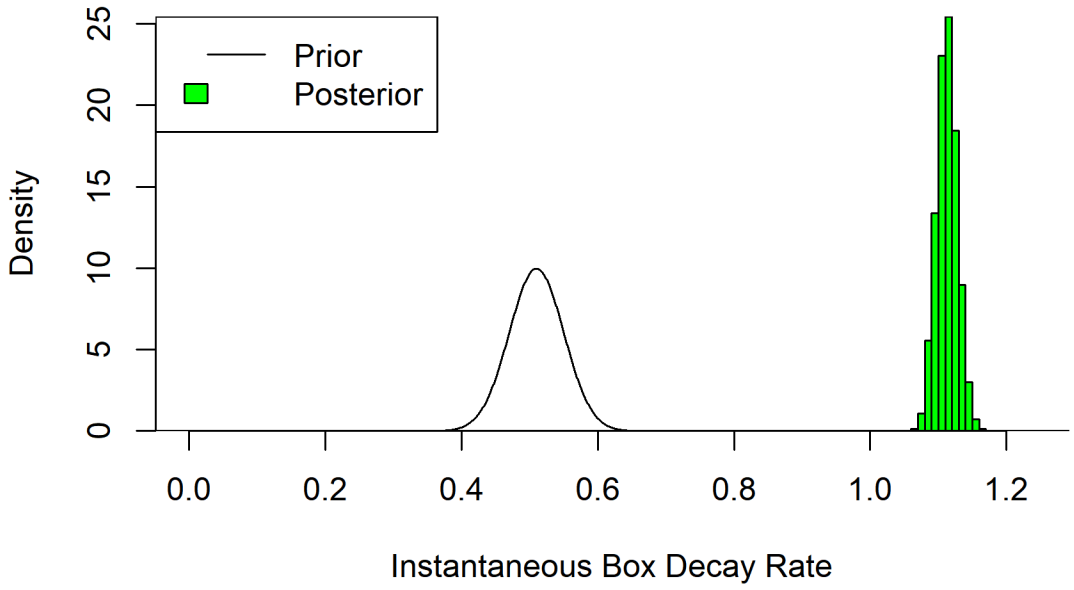

Figure 10. Prior (black line) and posterior (green histogram) distributions for the box decay (i.e., disarticulation) rate from the model.

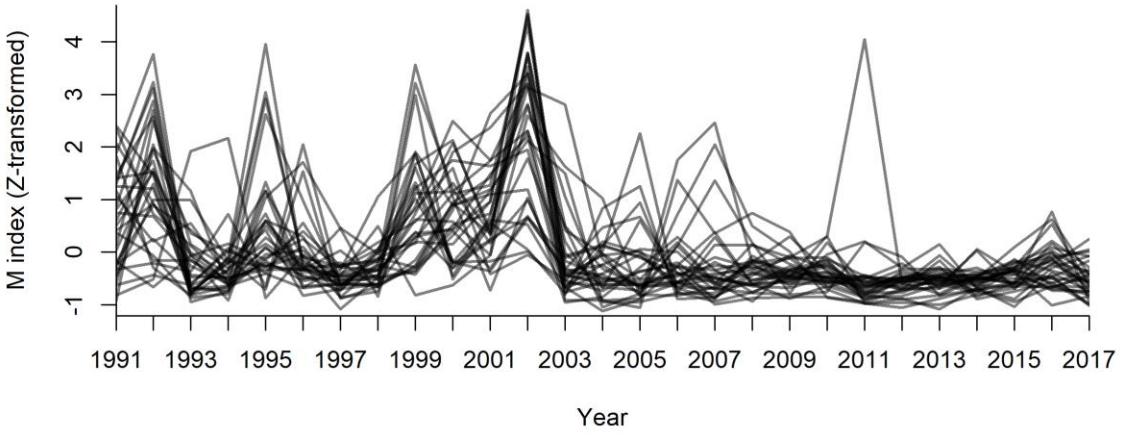

Figure 11. Standardized time series of median instantaneous natural mortality rates. Each line represents a time series of median instantaneous natural mortality for a NOAA code from the Bayesian model after subtracting the mean and dividing by the standard deviation of the time series. Lighter lines represent just one time series, whereas darker lines show where several time series have overlapping values.

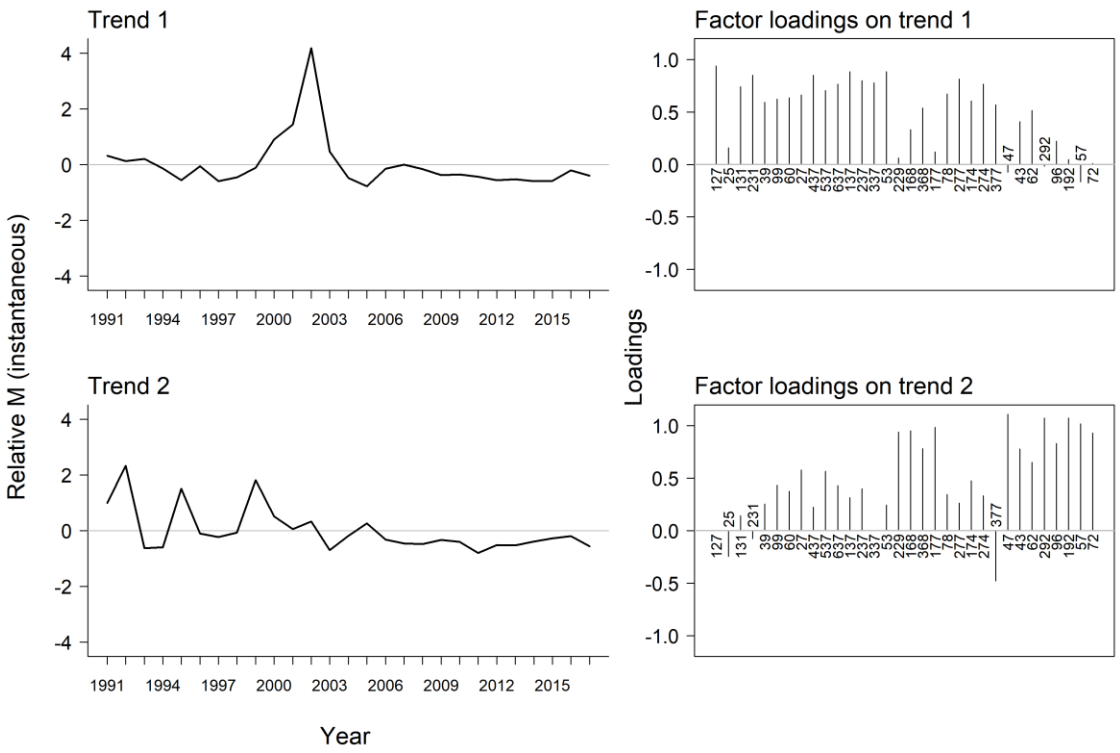

Figure 12. Trends and loadings from dynamic factor analysis with 2 trends. The labels on the factor loadings are NOAA codes, ordered by regions generally from north (left) to south (right). See table 1 for NOAA code names.

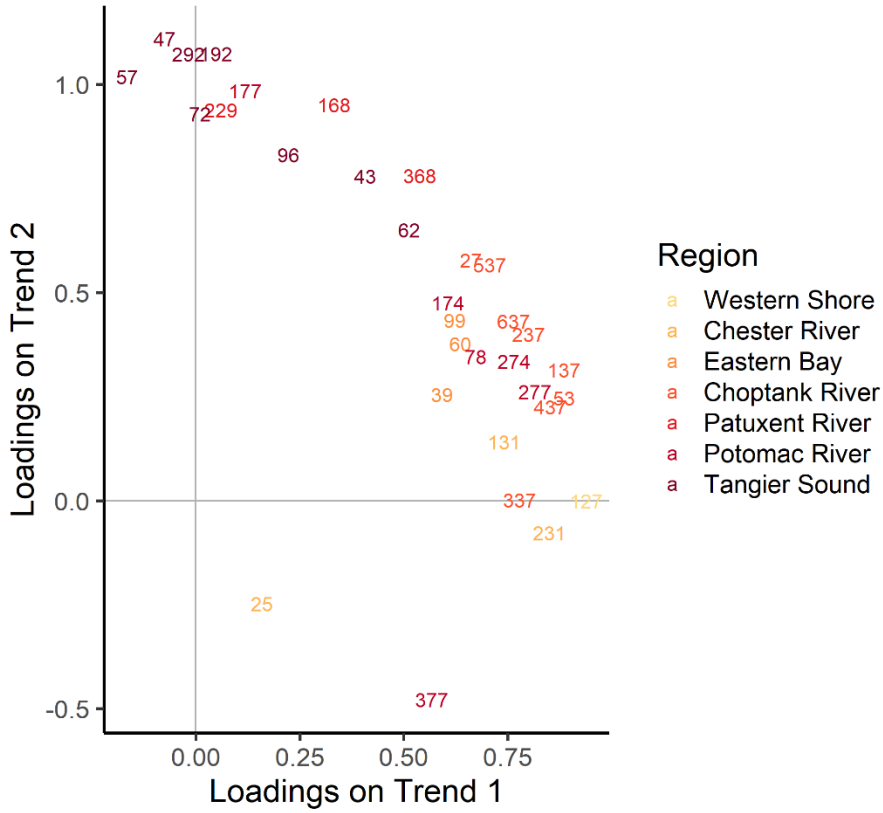

Figure 13. Loadings from dynamic factor analysis with two trends. The NOAA code numbers are plotted at the location of their loadings, and their color indicates the region of the NOAA code, where more northernly NOAA codes have lighter colors than more southernly NOAA codes. See table 1 for NOAA code names.

Chapter 2: Do the relationships of environmental factors, disease, and natural mortality for oysters in Chesapeake Bay, MD change spatially and/or temporally?

Introduction

Infectious marine diseases are increasing in some groups of marine organisms (Ward & Lafferty 2004) and are expected to continue to increase in frequency and severity in the future (Harvell et al. 2002, Burge et al. 2014). This trend is particularly problematic for fished species, because lethal infectious marine diseases can decrease abundance by increasing natural (i.e., non-fishing derived) mortality (e.g., Marty et al. 2010, Hoenig et al. 2017). Furthermore, infectious marine diseases affect the population dynamics of fished species including marine fishes like pacific herring *Clupea pallasi* (Marty et al. 2003, 2010) and striped bass *Morone saxatilis* (Gauthier et al. 2008, Hoenig et al. 2017), decapods like snow crab *Chionoecetes opilio* and American lobster *Homarus americanus* (Hoenig et al. 2017), and many mollusc species (Gulka et al. 1983, Arzul & Carnegie 2015).

The eastern oyster *Crassostrea virginica* has been susceptible to disease throughout most of its range in the last few decades (Burge et al. 2014), particularly to the diseases MSX and dermo, which are caused by the protozoan parasites *Haplosporidium nelsoni* and *Perkinsus marinus*, respectively. In the mid-Atlantic region of the U.S., these diseases cause epizootics resulting in mass mortality (Ford & Tripp 1996, Albright et al. 2007), which has likely fundamentally changed the population dynamics of these oyster

populations (Wilberg et al. 2011). The severity of mortality events due to MSX and dermo can fluctuate depending on environmental conditions, especially salinity and temperature. High salinity is typically correlated with increases in MSX and dermo disease levels (Bushek et al. 2012, Petes et al. 2012, Wang et al. 2012), whereas low salinity can suppress infections (Ford 1985, La Peyre et al. 2003). Thus, a gradient of MSX and dermo is typical in estuaries, where diseases are most prevalent or have the highest infection intensity in the highest salinity waters (Tarnowski 2017). In addition, salinity can vary interannually at the same estuarine location due to the amount of freshwater inflow, resulting in variability in disease levels among years (Bushek et al. 2012). Temperature is also considered an important factor for disease, with disease levels increasing at higher temperatures (Hewatt & Andrews 1956, Ford & Haskin 1982, Chu & La Peyre 1993). Temperature is correlated with the seasonal cycling of MSX and dermo in the mid-Atlantic region, where disease levels and disease mortality are highest during the warmest months and are depressed during the winter (Andrews & Hewatt 1957, Ford & Haskin 1982, Ford & Tripp 1996, Ford et al. 1999, Ragone Calvo et al. 2003, Audemard et al. 2006).

The relationships in the oyster disease system may change, as oysters can develop resistance to disease (Haskin & Ford 1979). Ford and Tripp (1996) define resistance as "the relative ability of an organism to avoid infection or to withstand the effects of disease". Resistance has been shown in some regions for MSX, but not for dermo. For example, in Delaware Bay and in the Virginia portion of Chesapeake Bay, resistance of oysters to MSX has been well documented (Haskin & Ford 1979, Carnegie & Burreson

2011, Bushek & Ford 2016). However, although stocks vary in their susceptibility to dermo (Bushek & Allen 1996, Brown et al. 2005a, Brown et al. 2005b, Encomio et al. 2005), resistance to dermo has not been clearly shown in the Mid-Atlantic region (Brown et al. 2005b, Bushek et al. 2012, Bushek & Ford 2016). Despite considerable research on disease resistance of wild oysters in nearby Delaware Bay and the Virginia portion of Chesapeake Bay, resistance to MSX by wild oysters has not been investigated in the Maryland waters of Chesapeake Bay.

The development of resistance could lead to changes in the relationships between environmental factors, disease prevalences, and disease mortality (the oyster disease system). Since 2003, natural mortality has been consistently low (chapter 1). This may be because favorable environmental conditions (i.e., low temperature and salinity) have allowed disease pressure to subside. It is also possible that disease resistance has developed, or both scenarios have worked in tandem to create low and stable mortality since 2003. Our objective was to examine spatial and temporal changes in the disease system of Maryland adult oysters during 1991-2017. We assessed if these relationships indicated the development of disease resistance. If oysters develop resistance to disease, then they may experience lower disease prevalences for the same temperature and salinity conditions compared to the past, or oysters could still experience high levels of disease, but a given prevalence may not result in the same natural mortality rate. If there were no clear changes, then it is likely that mortality has only been low and stable since 2003 because of favorable environmental conditions and not because of a change in the relationships in the oyster disease system.

Methods

We constructed structural equation models (SEMs) that specified causal relationships among temperature and salinity during the spring and summer, MSX and dermo prevalences in the fall, and natural mortality rates (which include disease mortality). Structural equation modeling (SEM) is used to estimate relationships among variables where causation is implied. Latent (i.e., unobserved) variables can also be included (SEM is also called path analysis when no latent variables are included). While it can be computationally similar to linear regression, the strengths of SEM are that it is a framework where causation is explicitly included and indirect effects (or mediation) can be estimated. In our analysis, the models had the same causal relationships but estimated parameters for different temporal and spatial groupings. We then used model selection criteria to select the best model among the suite of models and used the selected model to describe how relationships changed temporally or spatially in Maryland.

Study site: The Maryland portion of Chesapeake Bay

The Chesapeake Bay is a partially mixed estuary in the mid-Atlantic region of the U.S. Our study focused on the northern half of the bay that is part of Maryland (Figure 14). In general, the Maryland waters of Chesapeake Bay are less saline than the lower (Virginia) portion of the Bay, but the salinity gradient from the northern to the southern part of the Maryland portion of the bay is still substantial (approximately 6 to 17 on average among a subset of Maryland oyster bars) and varies interannually due to freshwater inflow. Oysters occur throughout Maryland's portion of Chesapeake Bay on subtidal bars in areas with average salinities > 5 (Maryland Department of Natural Resources 2016).

Data

Disease prevalences and natural mortality

Maryland Department of Natural Resources (MDNR) collects data each year on disease[3] as well as counts of live oysters and boxes per dredge tow during the oyster fall dredge survey (see Vølstad et al. 2008 or Tarnowski 2017 for a description of methods). At 43 fixed sites, 30 adult oysters are retained and assessed for MSX and dermo presence or absence, although sample sizes can be fewer than 30 if 30 oysters were not collected. Methods of assessing MSX and dermo disease have changed over time (for description of oyster disease analyses, see Tarnowski 2017). Prevalence (i.e., percent infected) at each bar and year for each disease was calculated.

Median annual natural mortality for each bar and year was taken from the Bayesian model (chapter 1). This model uses observations of live oysters and boxes (i.e., articulated oyster shells) to estimate rates of natural mortality on an annual time step. This model also includes corrections for differential dredge efficiency between live oysters and boxes, as well as for boxes persisting for more or less than one year. In this model, natural mortality was estimated on the NOAA code level (NOAA codes are statistical catch areas that typically include multiple bars), so bars were assigned natural mortality values based on NOAA codes (i.e., all bars in the same NOAA code were assigned the same time series of natural mortality).

[3] Maryland Department of Natural Resources, Fisheries Service, Cooperative Oxford Laboratory. (2018). MDNR Individual Oyster Disease Data, (1990 to 2017) [Dataset]

Temperature and salinity

Because continuous measurements of temperature and salinity during the season were not available over the entire time series (1991-2017) for the oyster bars included in our study, we used interpolated water temperature and salinity at the surface for the midpoint of each bar from the Chesapeake Bay Program Tidal Water Quality Monitoring data[4]. These data have been collected at least monthly year-round since 1984[5]. We used ordinary kriging to interpolate the surface (i.e., typically <1 m depth in the water column) water temperature and salinity values during each "cruise" (a simultaneous sampling effort across the bay that can span multiple days) at all sites in the tidal region of Chesapeake Bay (both Virginia and Maryland). Although oyster bars in Maryland are typically subtidal, surface water temperature and salinity should describe conditions experienced by oysters, as oyster bars likely can only persist long-term in regions of the bay that are well mixed. In addition, using surface data provides the most information for kriging because there are more observations for the surface than for other layers of the water column. On average, the difference in salinity between depths of 1 m and 4 m was only 1 (4.1 m is the average depth of oyster bars in the fall dredge survey).

Although the monitoring data should be collected at fixed sites at least once a month, sampling procedures differ in tributaries and the mainstem, and sites are not always sampled during each cruise. To ensure sufficient spatial coverage for kriging, we only used interpolations from cruises that had at least 5 samples taken in each of 3 general

[4]Data available from https://www.chesapeakebay.net/what/downloads/cbp_water_quality_database_1984_present.
[5] Dataset description at https://www.chesapeakebay.net/documents/3676/wq_data_userguide_10feb12_mod.pdf.

regions of Maryland: the western tributaries, eastern tributaries, and mainstem of Chesapeake Bay, Maryland (i.e., cruises had to have at least 15 samples total).

We followed ordinary kriging procedures outlined in Murphy et al. (2010) by using the R package automap (Hiemstra et al. 2009). In short, we considered several variogram functions, selected the sample variogram with the smallest residual sum of squares for each cruise and variable (water temperature or salinity), and used this variogram to perform ordinary kriging. Water temperature and salinity values were interpolated at the centroid locations of oyster bars that are sampled annually for disease (Figures A-1, A-2 for example kriging values). If the centroid of an oyster bar was outside of the range of the observations, then no estimate of the variable at that oyster bar was recorded for the cruise.

Because kriging allows interpolated estimates of salinity to be outside the range of observed values (i.e., salinity that is negative or > 35), estimates that were outside of this range were removed (4 values of 19,006 interpolated estimates). The removal of these four points did not greatly influence the summarized values of salinity. No values were removed from the temperature data set because unreasonable values were not identified.

We quantified water temperature and salinity at oyster bars as the average during April to October for each year. Monthly averages were obtained from the interpolated data sets by oyster bar, and values for the months from April to October were averaged. Field and modeling studies from the Mid-Atlantic region (Burreson & Ragone-Calvo 1996, Ford et

al. 1999, Paraso et al. 1999, Powell et al. 1999, Ragone Calvo et al. 2003, Audemard et al. 2006, Albright et al. 2007, Abbe et al. 2010) indicate that the April to October window encompasses the months when disease levels increase in the Chesapeake Bay.

Structural equation modeling

We compared nine structural equation models to investigate the importance of allowing relationships to vary temporally and spatially (Table 4). We modeled disease (MSX and dermo) prevalences as a function of environmental variables (temperature and salinity) and natural mortality as a function of disease prevalences (Figure 15). All relationships among variables were assumed to be linear with an estimated intercept. We compared models with different temporal groupings to determine if there was evidence for a change in these relationships over time perhaps due to the development of disease resistance, while spatial groupings were included to determine if there was any indication for difference in responses spatially. All models had the same structure but varied in their temporal and spatial groupings (i.e., different intercepts and slopes were estimated for the relationships for each temporal and/or spatial group combination). The R package lavaan (Rosseel 2012) was used to estimate parameters using a maximum likelihood framework.

We considered models with one, two, or four temporal groups and one to three spatial groups in all potential combinations. Models with one period included years 1991-2017, two periods were separated into 1991-2002 and 2003-2017, and four periods were separated into 1991-1997, 1998-2004, 2005-2011, and 2012-2017. Average salinity groups from the Maryland Oyster Management Review (Maryland Department of Natural Resources 2016) were used to group bars into spatial salinity categories. These categories

were high (>14 on average), medium (12 to 14), and low (5 to 11) salinity by NOAA code. Bars were assigned a salinity category (low, medium, or high) based on their NOAA code (Figure 14). For models with two spatial groups, the medium and high salinity zones were combined into one group.

Because our study focused on understanding how disease dynamics may have changed in Maryland over space and time, we removed other known natural mortality events from the dataset. In particular, freshets (pulsed freshwater events) can cause localized mass mortalities in oysters that are not disease related (MDNR 2001, Tarnowski 2012, Munroe et al. 2013). We used fall survey reports from MDNR (MDNR 2001, Tarnowski 2012) to determine years and locations where these freshets occurred (Table A-2) and did not include data from these bars and years in the model.

Models were compared using model selection criteria, including Akaike Information Criterion (AIC), Bayesian Information Criterion (BIC), sample-size corrected BIC (BIC2; Kuha 2004), sample-sized corrected AIC (AIC_C; Burnham and Anderson 2002), and Hannan-Quinn Information Criterion (HQC; Hannan and Quinn 1979) to determine which model had the best fit to the data. Only bars and years that had estimates of all variables were included in the models. We also used the absolute fit measures root mean squared error of approximation (RMSEA), standardized root mean squared residual (SRMR) and the comparative fit index (CFI) to compare fit among the models.

Results

Model selection and fit

Models that divided up both time and space performed better than those that did not by all model selection criteria (Table 5). However, the model selection criteria differed in their identification of the best model. AIC indicated that the model with four temporal groups and three spatial groups (model 9) was the best model, but BIC, BIC2, and HQC selected the model with two temporal and two spatial groups (model 6). AIC_C suggested that the model with two temporal groups and three spatial groups (model 7) should be chosen. Ultimately, we selected model 6, the model with two temporal (1991-2002 and 2002-2017) and two spatial (low and medium/high salinity) groups, because it was the most parsimonious among the models chosen by at least one model selection criterion, most of the model selection criteria suggested it was the optimal model, and among the models chosen by at least one model selection criterion, it had the best absolute model fit measures of RMSEA, SRMR, and CFI. For the selected model, the R^2 values ranged from 0.08 to 0.45 (Table 6).

Temperature, salinity, disease prevalence, and natural mortality

Average temperature during April-October was similar among bars and years, varying between 19.5 °C and 23.1°C (Table 7). Average salinity varied more than temperature, ranging from 3.1-19.2. On average across bars, salinity was lower in the low salinity zone group compared to the medium/high salinity zone group during 1991-2002 and 2003-2017. Within the salinity zone groups, average salinity was slightly lower during 2003-2017.

MSX prevalence was lower than dermo prevalence (Table 7), with averages across bars by temporal and spatial groups ranging from 0.7-15.7 % for MSX and 52.9-84.1 % for dermo. Both MSX and dermo prevalences were on average higher in the medium/high salinity zone group compared to the low salinity zone group in the same period and were higher during 1991-2002 than during 2003-2017 within the salinity zone groups.

Average natural mortality across bars by temporal and spatial group ranged from 14.6-38.6% (Table 7). Natural mortality was higher on average in the medium/high salinity zone group compared to the low salinity zone group in the same period. Within the salinity zone groups, mortality was higher on average across bars during 1991-2002 than 2003-2017.

MSX prevalence relationships with temperature, salinity, and natural mortality

The effect of average temperature during April-October on MSX prevalence was not consistent among groups (Figure 16; Table 8). During 1991-2002 in the low salinity zone group, temperature had a positive effect on MSX, while during 2003-2017 in the medium/high salinity group, there was a negative effect. During 2003-2017 in the low salinity zone group and 1991-2002 in the medium/high salinity zone group, there was no effect, with 95% confidence intervals (CIs) that overlapped with zero.

Average salinity during April to October had a positive effect on MSX prevalence, with 95% CIs that did not include zero (Figure 16; Table 8). The size of the effect was larger in the medium/high salinity zone group compared to the low salinity group during the

same period. Within both the low and medium/high salinity zone groups, the size of the effect declined over time, indicating that in the later period, MSX prevalence would not increase as much for the same increase in salinity.

Estimates of the intercepts for MSX prevalence were -58.8 ± 20.0 % during 1991-2002 in the low salinity zone group and 44.8 ± 15.4 % during 2003-2017 in the medium/high salinity zone group (Table 9). In the other two groups, the intercepts were not significantly different from zero.

MSX prevalence had a positive effect on natural mortality in all groups, except during 2003-2017 in the low salinity region (95% CIs included zero; Figure 16; Table 8). In both low and medium/high salinity zone groups, the amount of mortality per unit MSX prevalence decreased over time, and there was no difference between the amount of mortality per unit MSX prevalence in different salinity zone groups during the same period (overlapping 95% CIs).

Estimates of the intercept for natural mortality during 2003-2017 in the low salinity zone group and the medium/high salinity zones group were 4.80 ± 1.28 % and 4.93 ± 1.36 %, respectively (Table 9). The intercepts for both salinity zone groups during 1991-2002 were not significantly different from zero.

Dermo prevalence relationships with temperature, salinity, and natural mortality

There was no clear effect of temperature on dermo prevalence in most cases, except during 1991-2002 in the low salinity zone group (Figure 16; Table 8) in which temperature had a positive effect on dermo prevalence. The effect of temperature on dermo had 95% CIs that overlapped zero for all other groups.

Salinity had a positive effect on dermo prevalences for all groups (Figure 16; Table 8), but temporal change in the effect of salinity on dermo differed spatially. For the low salinity group, the size of the salinity effect remained approximately the same over time, whereas it increased over time in the medium/high salinity group. Across regions, the effect was larger in the low salinity group compared to the medium/high salinity group during 1991-2002, but effects were similar in size during 2003-2017.

Estimates of the intercept for dermo prevalence was -154.5 ± 51.5 % during 1991-2002 in the low salinity zone group (Table 9). Intercepts for all other groups were not significantly different from zero (95% CIs overlapped zero).

Dermo prevalence had a positive effect on natural mortality in all groups (Figure 16; Table 8). Mortality per prevalence may have decreased for dermo in both salinity groups, although the 95% CIs are overlapped within the salinity zone groups. There was no difference between the amount of mortality per dermo prevalence during the same period but in different salinity groups.

Discussion

The oyster disease system appears to have changed over time in Maryland. The same MSX prevalence resulted in less mortality in both salinity zone groups during 2003-2017 relative to 1991-2002, which is expected if oysters have developed resistance to MSX. Given that resistance to MSX has been documented in both Delaware Bay and the highest salinity waters of Chesapeake Bay, Virginia (Haskin & Ford 1979, Carnegie & Burreson 2011, Ford & Bushek 2012, Bushek & Ford 2016), it is not surprising that oysters in Maryland also show similar signs of resistance to MSX.

We also found somewhat weaker support for the development of resistance to dermo (than to MSX) in Maryland during 2003-2017. Dermo-resistant oysters (i.e., oysters that experienced less mortality for the same prevalence) from Tangier Sound in the most saline part of the Maryland portion of Chesapeake Bay were found during 1999-2001, although oysters from the Choptank region did not have dermo resistance (Encomio et al. 2005). Interestingly, our results suggest that higher resistance may have developed since 2003, and that both low and medium/high salinity zones of Maryland may have developed some resistance to dermo over time. To our knowledge, no studies have investigated resistance to dermo in Chesapeake Bay during 2003-2017, and our results suggest that dermo resistance for oysters in Maryland is worth reinvestigating. There has been disagreement in the literature about the ability of oysters to develop resistance to dermo in the mid-Atlantic region (Bushek & Allen 1996, Yu et al. 2011, Bushek et al. 2012, Powell et al. 2012, Bushek & Ford 2016).

The model selection criteria indicated strong evidence that allowing for both temporal and spatial change when examining the oyster disease system in Maryland is important, as models with multiple temporal and spatial groups described the data better than models with less complexity. In Delaware Bay, relationships between dermo intensity and mortality differ spatially (Bushek et al. 2012), which demonstrates the importance of allowing for spatial differences in parameters associated with disease. Similarly, studies that found the development of MSX resistance (Haskin & Ford 1979, Carnegie & Burreson 2011, Ford & Bushek 2012, Bushek & Ford 2016) demonstrate the need for allowing for temporal changes. However, most studies on oyster disease have not attempted to estimate changes in relationships over time because of limited temporal and spatial scope. A strength of this study was a 27-year time series over a wide spatial area that allowed us to estimate spatiotemporal change in disease-associated parameters.

Low salinity regions in both Delaware Bay and the Virginia portion of Chesapeake Bay provide refuge from MSX, and consequentially inhibited the development of disease resistance to some extent (Carnegie & Burreson 2011, Ford & Bushek 2012, Bushek & Ford 2016). We did not find substantial differences between salinity zone groups in the changes in the MSX-mortality (or dermo-mortality) relationships, which suggests that low salinity regions included in our study may not serve as refuges. It is possible that regions of lower salinity than were included in our study could provide such a refuge. However, it is also possible that the spatial groups included in the model may not be at the appropriate spatial scale to detect refuges. A further complication is that refuges are

ephemeral due to salinity variability, meaning refuges and non-refuges are more of a continuum than two clearly distinct categories (Ford et al. 2012).

Salinity was more important than temperature in driving disease dynamics for most temporal and spatial groups. While temperature is an important driver of the seasonal cycling of diseases in the mid-Atlantic region (Andrews & Hewatt 1957, Ford & Haskin 1982, Ragone Calvo et al. 2003, Audemard et al. 2006), interannual variability in temperature did not have a large effect on disease prevalences, as in most spatiotemporal groups, the temperature-prevalence coefficient was not different than zero. Conversely, salinity consistently had a positive effect on disease prevalences. Salinity has been shown to affect oyster diseases in a number of systems (Mackin 1956, La Peyre et al. 2003, Pollack et al. 2011, Bushek et al. 2012). In Delaware Bay salinity modulates the interannual variability in disease levels, while temperature is important for the seasonal cycling of the disease (Paraso et al. 1999).

The direction of change over time in the salinity-prevalence relationship differed between MSX and dermo. The effect of salinity on MSX prevalence decreased over time in both spatial groups, but the effect of salinity on dermo prevalence remained the same in the low salinity zone group and increased over time in the medium/high salinity zones group. Differences between the diseases may account for these results. One difference between the diseases is the way they are transmitted. Dermo transmission primarily occurs through oysters filtering infective *P. marinus* cells in the water column that originated either from the tissue of deceased oysters or to a lesser degree from the pseudofeces and

feces of other oysters (Bushek et al. 2002, Ragone Calvo et al. 2003, Audemard et al. 2006). Less is known about the transmission of MSX. Initial infections start on the gills, suggesting the infection is likely acquired from an unknown infectious stage present in the water (Farley 1967, 1968, Ford & Tripp 1996, Sunila et al. 2000). However, unlike for dermo, for MSX there may be an unknown organism that serves as a reservoir for MSX infective cells or aids in transmission of MSX (Ford & Haskin 1982, Ford & Tripp 1996, Sunila et al. 2000). The changes in the relationship between salinity and MSX prevalence could be caused by changes in the abundance of an alternate host species. A large number of copies of *H. nelsoni* DNA were present in tunicates, *Styela* sp., suggesting they could be the unknown MSX reservoirs or transmission aides (Messerman & Bowden 2016). Another difference between MSX and dermo that may account for the difference in the direction of change for salinity-prevalence relationships is that different genes are associated with resistance to MSX and resistance to dermo and can be selected on differentially. It has not been possible to breed oysters that are both highly resistant to MSX and dermo, suggesting resistance to these diseases are not linked (Burreson 1991, Frank-Lawale et al. 2014). In addition, genetic modeling of resistance development suggest that MSX likely has one locus that is the most influential for the development of resistance due to its fast development of resistance (Munroe et al. 2015), while dermo may have many loci that are approximately equally influential (Powell et al. 2011). Finally, the virulence of the parasites that cause MSX and dermo can change over time, and not necessarily in the same way. Changes in virulence of parasites may affect the salinity-prevalence relationships and/or the prevalence-mortality relationships.

We did not account for direct effects of salinity and temperature on natural mortality in the models because we wanted to focus on changes in the disease system and because the number of oysters dying directly from salinity or temperature extremes is likely a small portion of the Maryland population. While freezing temperatures can kill intertidal oysters that are exposed, this analysis only looked at subtidal oyster bars that had an average depth of 4.1 m. Oysters are also tolerant of high temperatures (Shumway 1996), and oysters on subtidal reefs in Maryland are unlikely to be exposed to lethal temperatures (maximum and minimum kriged temperature estimates at oyster bars included in this analysis were 0.02°C and 31.1°C, respectively). Low salinity can also directly kill oysters on subtidal reefs in Maryland and can cause significant mortality (MDNR 2001, Tarnowski 2012), but these freshet localized mass mortality events are well documented. We removed data that may have included freshet-caused mortality because the focus of our study was on how the oyster disease system has changed over time.

It is also possible that salinity and temperature can affect mortality indirectly as mediated by predators rather than MSX and dermo parasites. However, we could not account for the potential change in predation rate due to salinity and temperature in the structural equation models. Oyster drills (several species of predatory gastropods) are among the few predators in Maryland that can kill adult oysters and are most active at high salinities and temperatures (White & Wilson 1996). The approximate abundance of fouling organisms (including oyster drills) in dredge samples are recorded during the MDNR fall

dredge survey, so these data could potentially be incorporated into the modeling to account for differential predation mortality temporally and spatially.

We used disease prevalence in the fall as a proxy of annual disease pressure, but this may not fully capture disease pressure because it only provides a snapshot of disease in the fall and because it does not include a measure of intensity or severity. Seasonal disease cycles may vary among years (Ragone Calvo et al. 2003, Audemard et al. 2006), but we could not include these intra-annual dynamics in the models because disease data is only collected during the fall in Maryland. For example, where MSX and dermo co-occur, MSX can have several peaks in intensity during the year (Andrews 1982), and one of the peaks in MSX sometimes occurs before a peak in dermo (Ragone Calvo et al. 2003, Audemard et al. 2006). When MSX causes widespread mortality before dermo (due to a peak in disease intensity), there are less oysters available to die and spread infective dermo particles (Ragone Calvo et al. 2003). Oysters can also acquire MSX and dermo concurrently (Sunila et al. 2000, Ragone Calvo et al. 2003), but the effect of oysters having both diseases is not well characterized. The disease level can also be quantified differently in the structural equation models; for example, infection intensity could be used instead of prevalence (e.g., Albright et al. 2007, Abbe et al. 2010, Bushek et al. 2012). We did not include a measures of infection intensity in the models because methods to assess MSX intensity have changed over time.

Natural mortality rates estimated on the NOAA code level were applied to all bars within the NOAA code, and thus the analysis ignores among bar variability within a NOAA

code. To address the different spatial scales between the NOAA code level estimates of natural mortality and the bar-level estimates of temperature, salinity, and disease prevalences used in the structural equation models, the analyses could either be conducted on the NOAA code level for all data, or the natural mortality could be modified to estimate bar-level natural mortality. Of these two options, using bar-level estimates of natural mortality would provide the best alignment between the model assumptions and the data. If natural mortality rates are similar among bars within a NOAA code, then the results of the analysis would not change; however, natural mortality rates varying substantially among bars within a NOAA code could change the results of the analysis.

We had to choose spatial categories to group the data for the models. We chose salinity to create spatial groupings, as we thought that if refuges from disease existed, they would occur based on average salinity regimes. The salinity zones from Maryland Department of Natural Resources (2016) were one approach to define groups by salinity, although other salinity groupings are possible. The methods to create these salinity groupings were not specified in the report, and thus it is possible the salinity zones are not relevant to the modeled years. Furthermore, the salinity zones were created for NOAA codes, and thus by applying these groupings to bars, there could be some misclassifications.

We also had to choose temporal breakpoints to group the data. We chose the breakpoints in the time series for two reasons: to break the time series into nearly even lengths of time and because of the high mortality events during 1999-2002. We thought that if resistance

to either MSX or dermo had developed in a short time frame due to a selective event, it would have developed after 2002, and therefore we would see evidence of resistance if we broke the times series between 2002 and 2003. For models with three breakpoints (four temporal groups), we further divided time series as evenly as possible between 1991 and 2002, and 2003 and 2017. Other breakpoints could be possible, but 2002 was estimated as the best year for a single breakpoint (based on relative model fit) in a subsequent analysis in which the 2 temporal and 2 spatial group SEM was implemented varying the breakpoint year (breakpoints tested were every other year during 1996-2014).

Another choice in the analysis was how to summarize environmental data in a way that is relevant to oyster disease. We chose average warm weather temperature and salinity because they are simple, relevant metrics that were possible to calculate with the temporal resolution of the kriged salinity and temperature estimates. Other possibilities include using degree days or specifying the number of observations where temperature or salinity were above or below a biological threshold for the effects of disease on oysters. Using either technique could be challenging due to the temporal resolution of the environmental data (observations were collected only 1 – 2 times per month). Furthermore, relationships could be non-linear (e.g., an exponential relationship between temperature and prevalence), which would be difficult to implement within the R package lavaan. Experimental studies and syntheses have provided insight into potential temperature and salinity thresholds for MSX and dermo (Hewatt & Andrews 1956, Ford & Haskin 1982, Ford 1985, Chu & La Peyre 1993, Chu et al. 1993), but using this information within our modeling framework would also be difficult.

Previous oyster disease studies have found high winter temperature correlated with high MSX disease levels the following year (e.g., Ford & Haskin 1982, Bushek et al. 2012). Using average winter temperature (i.e., temperature during January and February) instead of warm weather temperature in our analysis had no qualitative effect on the changes in coefficients among spatial and temporal groups. Additional sensitivity analyses of changing the months of data included in the averages of temperature and salinity could be conducted to understand the effect of our chosen temperature and salinity windows on the analysis.

Another limitation of the analysis is that it was not possible to include estimates of uncertainty in natural mortality in the SEMs. Output from the Bayesian natural mortality model (chapter 1) was treated as data in the SEMs. Similarly, we used estimates of temperature and salinity that were derived from kriging. Using model estimates as data can be problematic because the uncertainty in the estimates is not promulgated through the analyses, which can cause conclusions to be overstated (Brooks & Deroba 2015). To improve the analysis, the uncertainty of the estimates could be included when fitting the structural equation models, or both the estimation of natural mortality and fitting of structural equation models could be done within the same framework. Including uncertainty was not done because it could not be implemented in the R package lavaan that we used to fit the SEMs.

Our analysis estimated change in the environment-disease-mortality relationships for oysters in Maryland and suggests that both environmental conditions and potential changes in how oysters resist disease are important to consider when trying to predict mortality from disease. In particular, natural mortality rates have been low since 2003 (chapter 1) likely not just because of good environmental conditions (i.e., high rainfall resulting in lower than normal salinity), but also because oysters appear to have developed resistance to MSX. This resistance is indicated by a decrease in the natural mortality at a given level of MSX prevalence and possibly by a reduction in the level of prevalence at a given salinity. Thus, lower mortality levels from MSX may be expected into the future in Maryland barring additional changes in this complex disease system. These results are encouraging because oyster recovery may not be possible without decreases in disease-related natural mortality (Mann & Powell 2007).

Tables

Table 4. Structural equation models compared, with their associated temporal and spatial groups. These models have the same structure (outlined in Figure 15) and only differ in the number of spatial and temporal groups (shown in the number of temporal/spatial groups columns). The temporal groups (years) column shows the year range for each temporal group, while the spatial groups (salinity zones) columns shows how the data were divided up into spatial groups using salinity zones. The total number of groups column shows the number of separate models estimated due to the number of spatial and temporal groups used to divide up the data.

Model number	Number of temporal groups	Temporal groups (years)	Number of spatial groups	Spatial groups (salinity zones)	Total number of groups
1	1	1991-2017	1	All zones together	1
2	2	1991-2002, 2003-1997	1	All zones together	2
3	4	1991-1997, 1998-2004, 2005-2011, 2012-2017	1	All zones together	4
4	1	1991-2017	2	Low and Medium/High	2
5	1	1991-2017	3	Low, Medium, and High	3
6	2	1991-2002, 2003-2017	2	Low and Medium/High	4
7	2	1991-2002, 2003-2017	3	Low, Medium, and High	6
8	4	1991-1997, 1998-2004, 2005-2011, 2012-2017	2	Low and Medium/High	8
9	4	1991-1997, 1998-2004, 2005-2011, 2012-2017	3	Low, Medium, and High	12

Table 5. Model selection criteria and absolute fit measures for SEM models. The first three columns show model number (which corresponds with model numbers in Table 4) and the number of temporal and spatial groups included in the model, respectively. Model selection criteria are shown relative to the model with the lowest value and included Akaike information criterion (AIC), Bayesian information criterion (BIC), a sample size corrected Bayesian information criterion (BIC2), sample size corrected AIC (AIC_c), and Hannan-Quinn Information Criterion (HQC). Absolute fit measures included the root mean squared error of approximation (RMSEA), standardized root mean squared residual (SRMR), and the comparative fit index (CFI). The shaded row indicates the model chosen on the basis of the model selection criteria and relatively good fit measures.

Model number	Number of temporal groups	Number of spatial groups	ΔAIC	ΔBIC	ΔBIC2	ΔAICc	ΔHQC	RMSEA	SRMR	CFI
1	0	0	1488.05	1239.62	1353.96	1455.07	1352.62	0.07	0.02	0.99
2	2	0	649.83	461.92	538.15	617.65	537.26	0.11	0.03	0.96
3	4	0	662.00	595.12	595.12	633.03	595.12	0.14	0.04	0.95
4	0	2	1162.88	974.96	1051.19	1130.69	1050.30	0.09	0.03	0.97
5	0	3	1107.36	979.96	1018.08	1076.51	1017.63	0.10	0.03	0.97
6	2	2	66.88	0.00	0.00	37.92	0.00	0.12	0.04	0.94
7	2	3	23.45	77.61	1.37	0.00	2.27	0.15	0.04	0.92
8	4	2	76.80	251.99	99.53	61.32	101.32	0.17	0.05	0.92
9	4	3	0.00	417.26	112.34	8.50	115.91	0.21	0.06	0.88

Table 6. R^2 for each group and variable and number of observations per group for the selected model (model 6; 2 temporal and 2 spatial groups). The years and salinity columns indicate the temporal and spatial classifications of the group, while the columns MSX Prevalence, Dermo Prevalence, and Mortality indicate R^2 values for their respective variables. The number of observations indicates the number of points (observations of temperature, salinity, disease prevalences, and natural mortality for one bar in one year) included in each of the temporal and spatial groups.

Years	Salinity Zone	MSX Prevalence	Dermo Prevalence	Mortality	Number of observations
1991-2002	Low	0.22	0.26	0.45	241
2003-2017	Low	0.11	0.08	0.20	329
1991-2002	Medium/High	0.33	0.11	0.39	246
2003-2017	Medium/High	0.20	0.18	0.24	329

Table 7. Mean, median, minimum, and maximum of temperature, salinity, disease, and mortality data used in the models by model 6 (2 temporal and 2 spatial groups). These were calculated by grouping the model input values for each variable (Variable column) by temporal (years) and spatial (salinity zone) groups, then calculating each measure (mean, median, minimum, and maximum) using the data for each group.

Years	Salinity Zone	Variable	Mean	Median	Minimum	Maximum
1991-2002	Low	Temperature	21.6	21.6	19.7	23.0
2003-2017	Low	Temperature	21.4	21.4	19.5	23.0
1991-2002	Medium/High	Temperature	21.6	21.5	19.9	23.1
2003-2017	Medium/High	Temperature	21.5	21.4	19.5	23.1
1991-2002	Low	Salinity	10.4	10.3	3.5	17.1
2003-2017	Low	Salinity	9.5	9.8	3.1	15.5
1991-2002	Medium/High	Salinity	12.9	13.3	6.4	19.2
2003-2017	Medium/High	Salinity	12.6	12.6	5.7	18.2
1991-2002	Low	MSX Prevalence	4.4	0.0	0.0	60.0
2003-2017	Low	MSX Prevalence	0.7	0.0	0.0	26.7
1991-2002	Medium/High	MSX Prevalence	15.7	6.7	0.0	100.0
2003-2017	Medium/High	MSX Prevalence	5.5	0.0	0.0	60.0
1991-2002	Low	Dermo Prevalence	76.1	86.7	0.0	100.0
2003-2017	Low	Dermo Prevalence	52.9	53.3	0.0	100.0
1991-2002	Medium/High	Dermo Prevalence	84.1	90.0	6.7	100.0
2003-2017	Medium/High	Dermo Prevalence	63.2	70.0	0.0	100.0
1991-2002	Low	Mortality	29.9	27.9	0.9	89.6
2003-2017	Low	Mortality	14.6	10.3	0.3	62.2
1991-2002	Medium/High	Mortality	38.6	35.5	0.6	96.1
2003-2017	Medium/High	Mortality	16.1	15.1	0.4	74.8

Table 8. Coefficient estimates for the selected model (model 6; two temporal and two spatial groups). Years and salinity zone columns indicate the group for which the coefficient was estimated. For the relationship column, the coefficient is included with the variable on the left-hand side of the relationship to estimate the variable on the right-hand side. Asterisks to the left of the estimate indicate coefficients that were **not** significantly different from zero. SE is the standard error associated with the estimate, and Lower/Upper 95% CI are the lower and upper approximate 95% confidence intervals, respectively.

Years	Salinity Zone	Relationship	Estimate	SE	Lower 95% CI	Upper 95% CI
1991-2002	Low	Temperature -> % MSX Prevalence	2.009	0.949	0.148	3.870
2003-2017	Low	Temperature -> % MSX Prevalence	*-0.348	0.203	-0.745	0.049
1991-2002	Medium/High	Temperature -> % MSX Prevalence	*-2.383	1.602	-5.523	0.757
2003-2017	Medium/High	Temperature -> % MSX Prevalence	-2.930	0.731	-4.363	-1.496
1991-2002	Low	Salinity -> % MSX Prevalence	1.905	0.260	1.396	2.414
2003-2017	Low	Salinity -> % MSX Prevalence	0.376	0.059	0.260	0.491
1991-2002	Medium/High	Salinity -> % MSX Prevalence	4.200	0.385	3.446	4.954
2003-2017	Medium/High	Salinity -> % MSX Prevalence	1.876	0.214	1.457	2.296
1991-2002	Low	% MSX Prevalence -> % Mortality	0.796	0.089	0.621	0.971
2003-2017	Low	% MSX Prevalence -> % Mortality	*0.103	0.239	-0.366	0.571
1991-2002	Medium/High	% MSX Prevalence -> % Mortality	0.670	0.062	0.549	0.791
2003-2017	Medium/High	% MSX Prevalence -> % Mortality	0.347	0.060	0.230	0.465
1991-2002	Low	Temperature -> % Dermo Prevalence	8.305	2.444	3.515	13.094
2003-2017	Low	Temperature -> % Dermo Prevalence	*-1.795	2.377	-6.454	2.864
1991-2002	Medium/High	Temperature -> % Dermo Prevalence	*2.262	1.825	-1.315	5.840
2003-2017	Medium/High	Temperature -> % Dermo Prevalence	*1.755	2.253	-2.660	6.170
1991-2002	Low	Salinity -> % Dermo Prevalence	4.950	0.668	3.641	6.260
2003-2017	Low	Salinity -> % Dermo Prevalence	3.649	0.692	2.293	5.005
1991-2002	Medium/High	Salinity -> % Dermo Prevalence	2.074	0.438	1.215	2.933
2003-2017	Medium/High	Salinity -> % Dermo Prevalence	5.361	0.659	4.069	6.653
1991-2002	Low	% Dermo Prevalence -> % Mortality	0.287	0.034	0.221	0.354
2003-2017	Low	% Dermo Prevalence -> % Mortality	0.184	0.021	0.143	0.225
1991-2002	Medium/High	% Dermo Prevalence -> % Mortality	0.277	0.063	0.154	0.400
2003-2017	Medium/High	% Dermo Prevalence -> % Mortality	0.146	0.020	0.107	0.184

Table 9. Intercept estimates for the selected model (model 6; 2 temporal and 2 spatial groups). Years and salinity zone columns indicate the group for which the intercept was estimated, and the variable indicates the variable for which the intercept was estimated. Asterisks to the left of the estimate indicate intercepts that were not significantly different from zero. SE is the standard error associated with the estimate, and Lower/Upper 95% CI are the lower and upper approximate 95% confidence intervals, respectively.

Years	Salinity Zone	Variable	Estimate	SE	Lower 95% CI	Upper 95% CI
1991-2002	Low	MSX Prevalence	-58.79	20.01	-98.02	-19.57
2003-2017	Low	MSX Prevalence	*4.53	4.32	-3.94	13.01
1991-2002	Medium/High	MSX Prevalence	*12.69	33.40	-52.78	78.16
2003-2017	Medium/High	MSX Prevalence	44.84	15.38	14.70	74.98
1991-2002	Low	Dermo Prevalence	-154.50	51.51	-255.45	-53.55
2003-2017	Low	Dermo Prevalence	*56.66	50.74	-42.79	156.12
1991-2002	Medium/High	Dermo Prevalence	*8.40	38.06	-66.20	82.99
2003-2017	Medium/High	Dermo Prevalence	*-41.78	47.36	-134.59	51.04
1991-2002	Low	Mortality	*4.54	2.69	-0.72	9.81
2003-2017	Low	Mortality	4.80	1.28	2.28	7.31
1991-2002	Medium/High	Mortality	*4.89	5.31	-5.53	15.31
2003-2017	Medium/High	Mortality	4.93	1.36	2.25	7.60

Figures

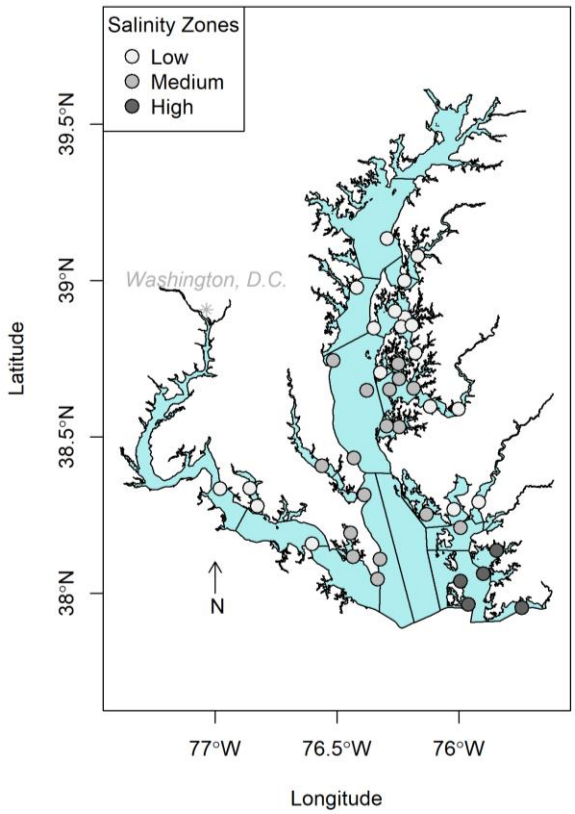

Figure 14. Map of Maryland portion of Chesapeake Bay showing location of oyster bars included in models. The circles represent the approximate location of the center of the oyster bars and are shaded gray based on the salinity zone category. The gray asterisk denotes the approximate location of Washington, D.C. for reference.

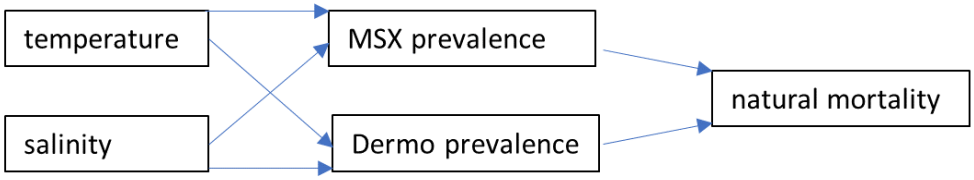

Figure 15. Path analysis diagram of structural equation models. Following standard path analysis diagram conventions, the boxes represent observed variables in the model. The arrows indicate the direction of the relationships, where the variable from which the arrow originates causes the variable to which the arrow is pointing. Intercepts, covariances, and residual variances are not illustrated here for clarity, but all relationships are assumed to be linear with an intercept.

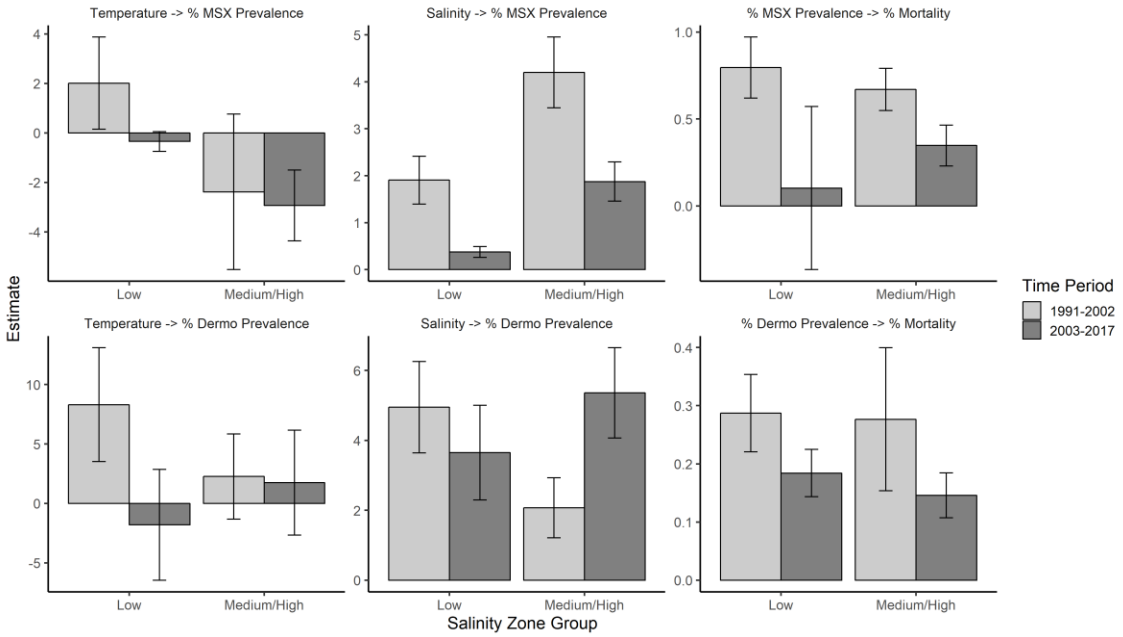

Figure 16. Coefficients (bars) of model relationships (plot titles) for the selected model, model 6 (2 temporal and 2 spatial groups). The error bars represent approximate 95% confidence intervals. The units for temperature are °C, for prevalences are percent infected, and for mortality are percent yr^{-1}. The units of the coefficients therefore are the units for the second variable of the relationship per the units of the first variable; for example, the units for the temperature affecting MSX relationship (top left) are percent infected $°C^{-1}$). Negative values indicate that there is an inverse relationship between the two variables.

Appendices

Appendix to Chapter 2

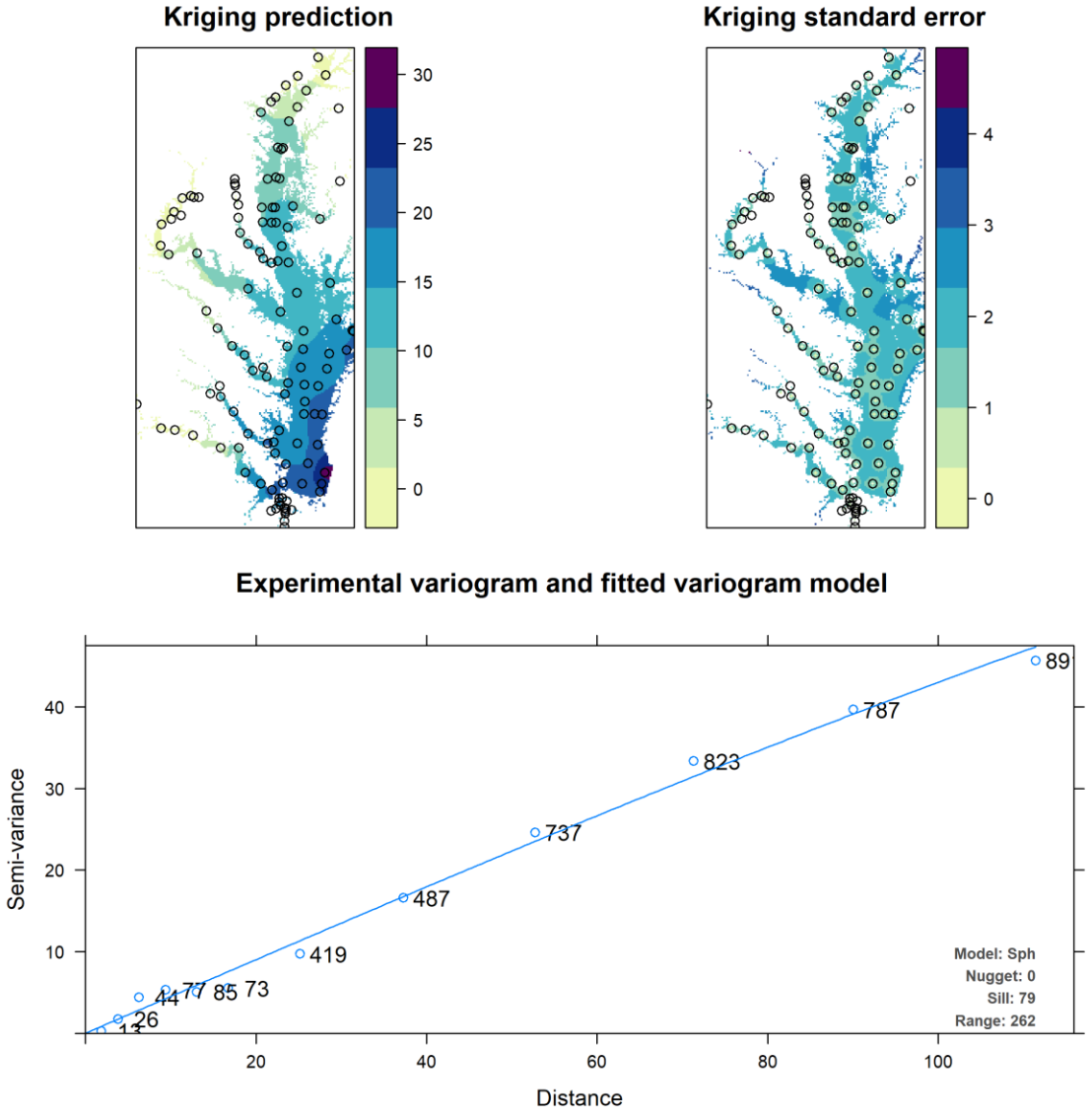

Figure 1-A. Example kriged data set for salinity, Cruise BAY282 (August 1998). The top row of figures show kriged point estimates (kriging prediction) and its associated standard error (kriging standard error) on maps of the Chesapeake Bay. The colors on the plots show the predictions of point estimates or standard error from kriging, while the black circles denote the location of samples used in kriging. The bottom row shows the experimental variogram (points) and the fitted variogram model (line) used in kriging. The text in the bottom right corner of the variogram plot shows the fitted variogram model form and its estimated parameters.

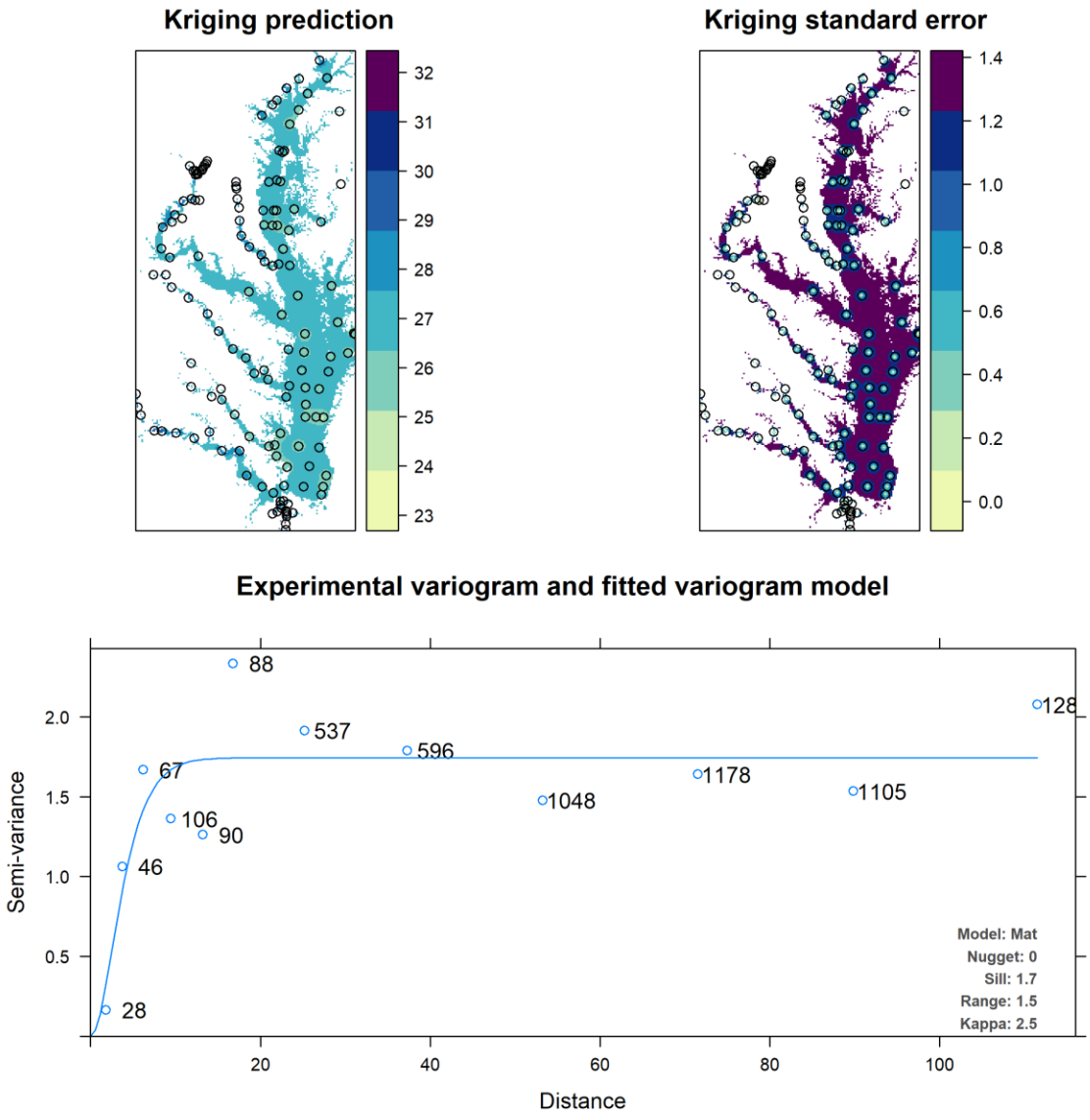

Figure 2-A. Example kriged data set for temperature (°C), Cruise BAY284 (August 1998). Symbol definitions are the same as appendix figure A-1.

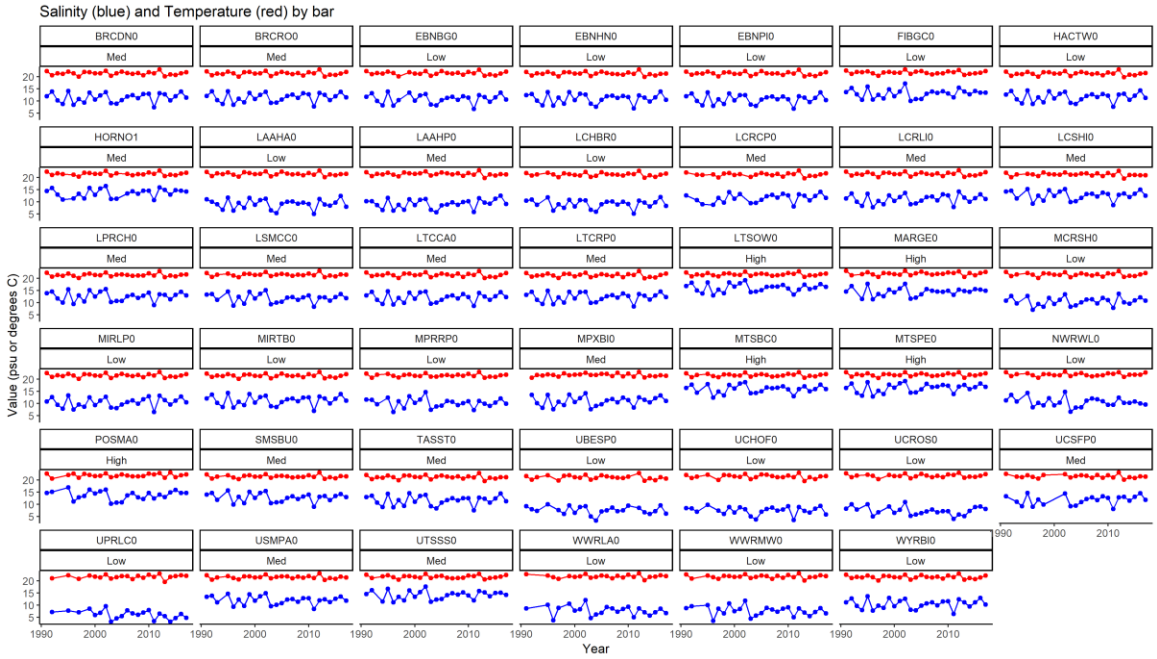

Figure 3-A. Average water temperature (°C) and salinity by oyster bar during March – October. Temperature estimates are shown in red, while salinity estimates are shown in blue. The boxes at the top of each plot show the bar name (top) and its salinity category (Low, Med, or High; bottom). All points in these plots were used as input for the structural equation models.

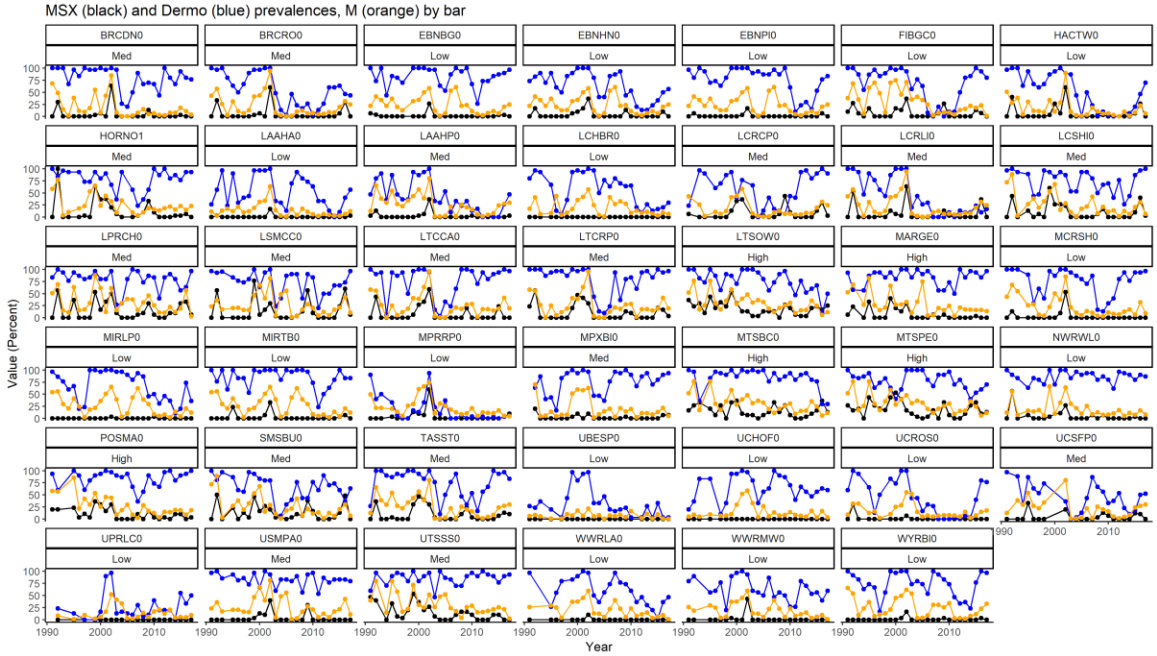

Figure 4-A. Fall disease prevalences and natural mortality. MSX prevalence is shown in black, Dermo prevalence is shown in blue, and natural mortality is shown in orange. The boxes at the top of each plot show the bar name (top) and its salinity category (Low, Med, or High; bottom). All points in these plots were used as input for the structural equation models.

Biplots:

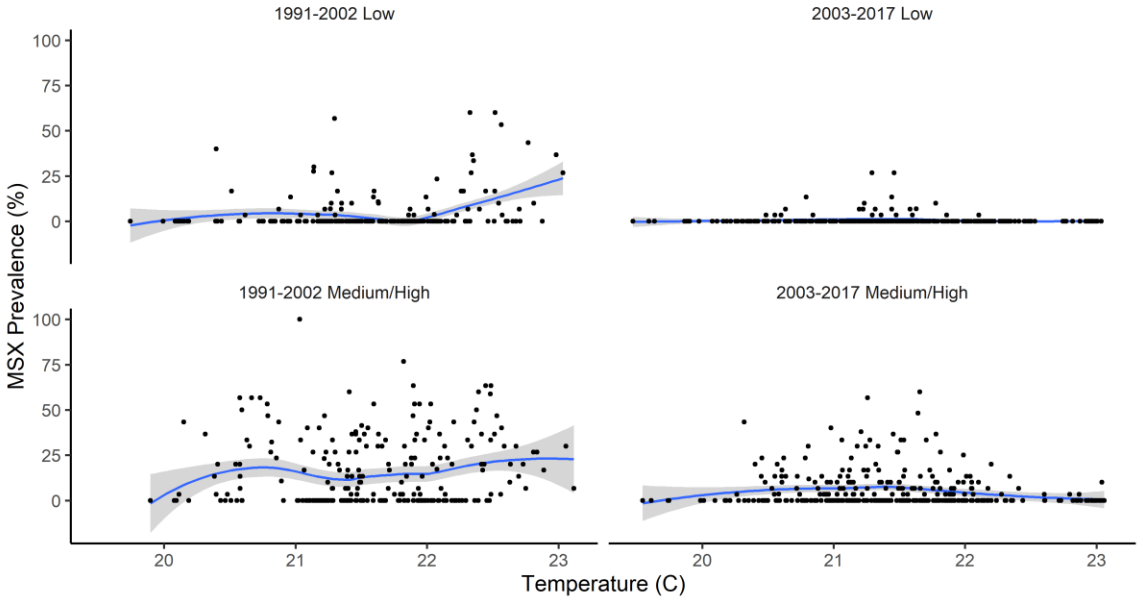

Figure 5-A. MSX prevalence (percent infected) versus temperature (°C). Points denote observations of MSX prevalence and temperature at a bar in a year. These were plotted separately according to the spatial and salinity groups in the selected model (model 6, 2 temporal and 2 spatial groups). The temporal (years) and spatial (salinity zone) group is shown in the title of each plot. The line and shaded area are loess curves and estimated uncertainty.

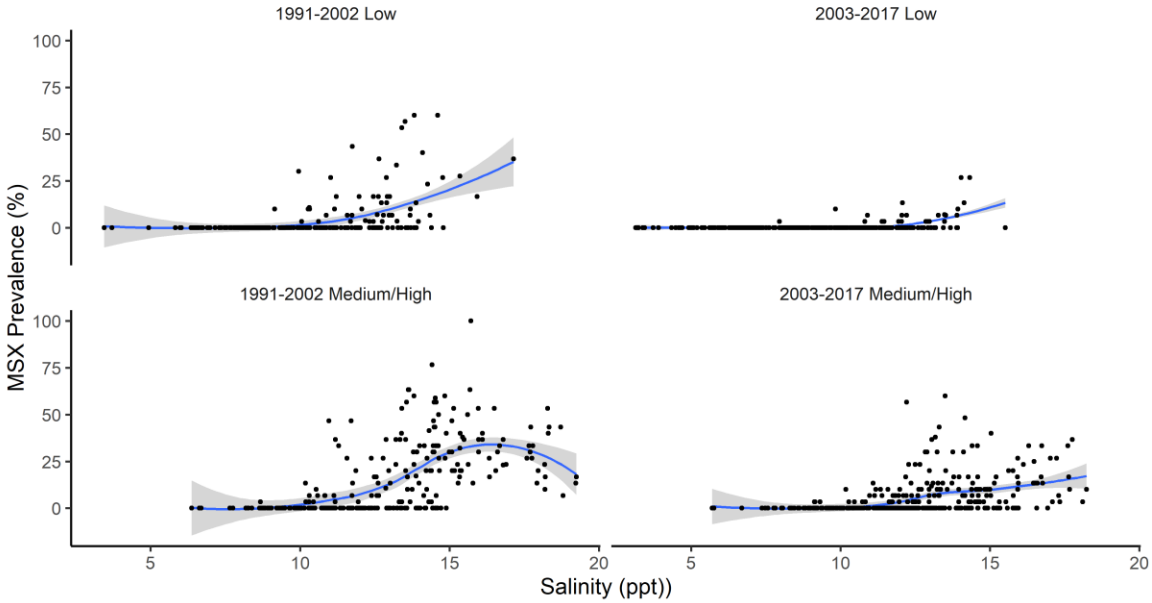

Figure 6-A. MSX prevalence (percent infected) versus salinity. Symbol definitions are as in Figure 5-A.

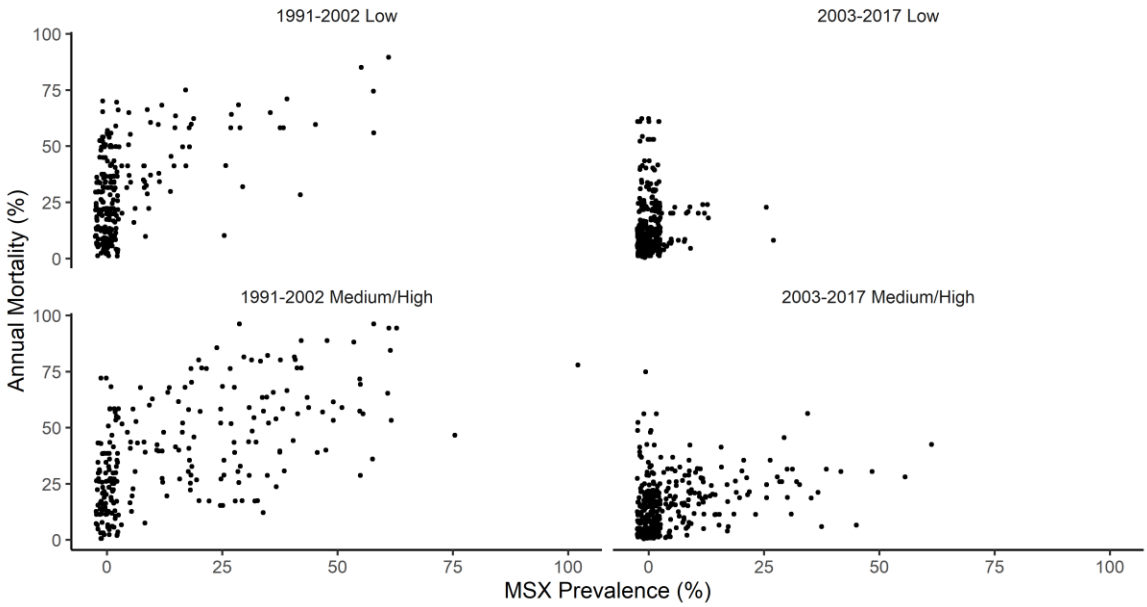

Figure 7-A. Natural mortality (percent yr^{-1}) versus MSX prevalence (percent infected). Symbol definitions are as in Figure 5-A, but a loess curve and uncertainty was not estimated, and a small amount (5%) of random noise was added to the data to reveal overlapping points.

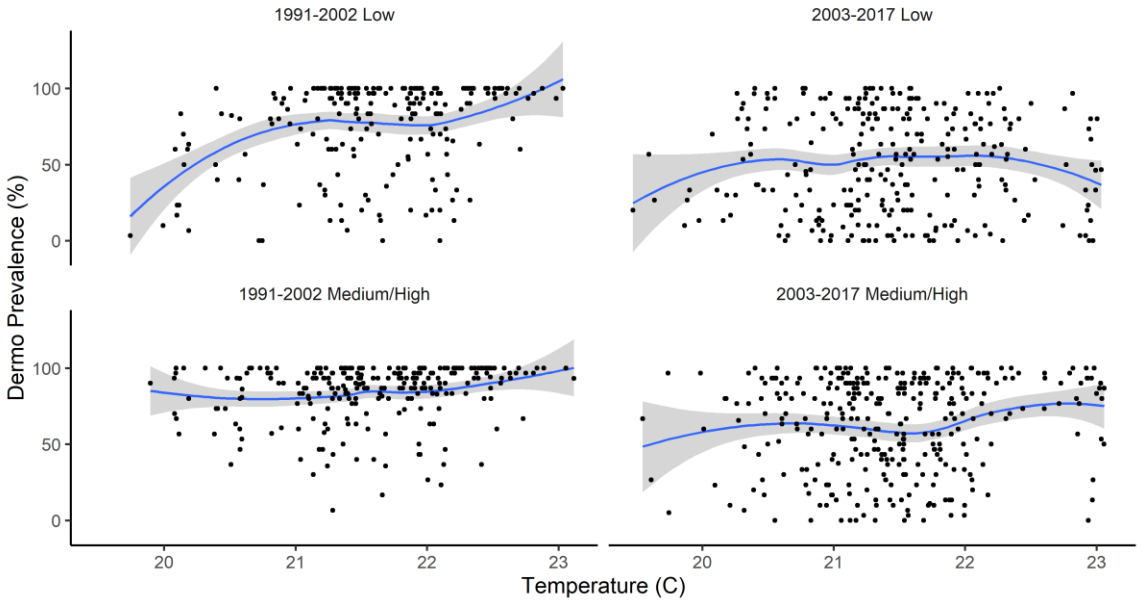

Figure 8-A. Dermo prevalence (percent infected) versus temperature (°C). Symbol definitions are as in Figure 5-A.

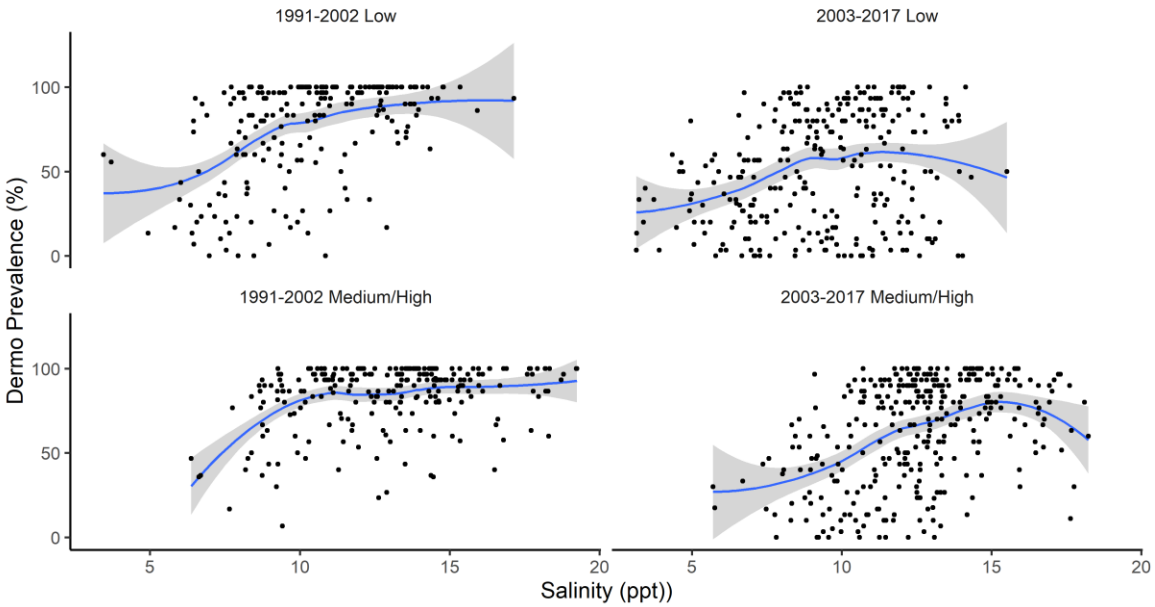

Figure 9-A. Dermo prevalence (percent infected) versus salinity. Symbol definitions are as in Figure 5-A.

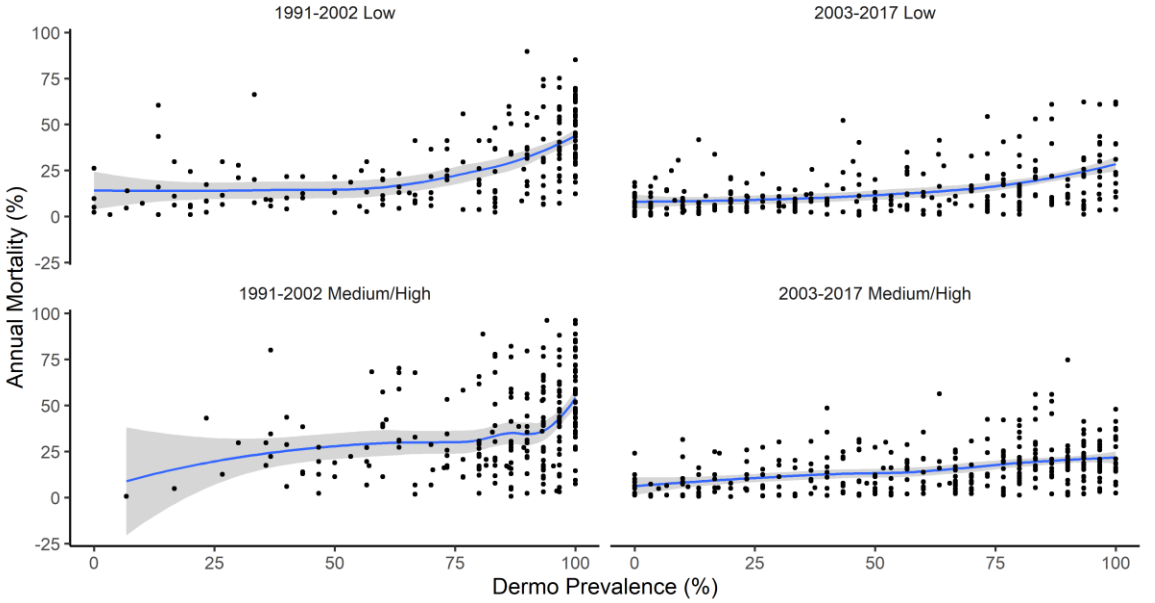

Figure 10-A. Natural mortality (percent yr^{-1}) versus dermo prevalence (percent infected). Symbol definitions are as in Figure 5-A.

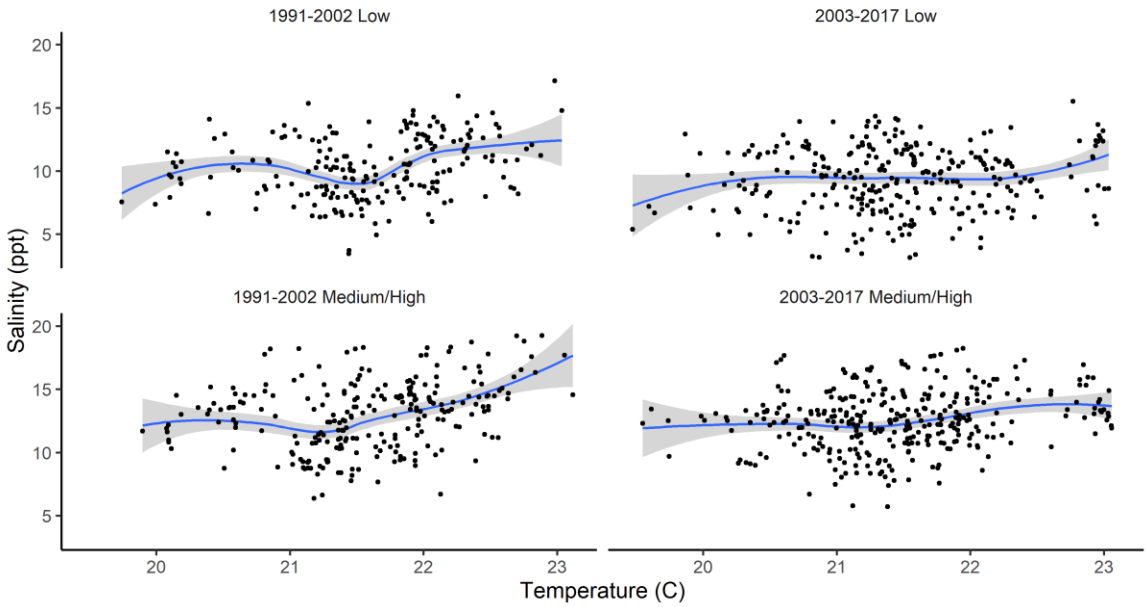

Figure 11-A. Salinity versus temperature (°C). Symbol definitions are as in Figure 5-A.

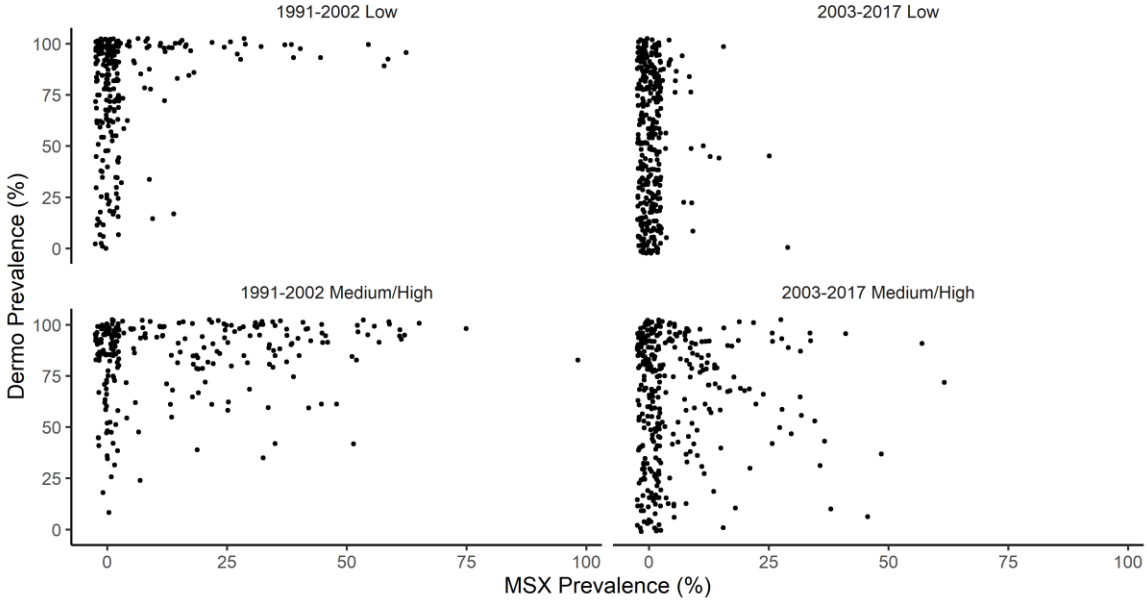

Figure 12-A. Dermo prevalence (percent infected) versus MSX prevalence (percent infected). Symbol definitions are as in Figure 5-A, but a loess curve and uncertainty were not estimated, and a small amount (5%) of random noise was added to the data to reveal overlapping points.

Table 1-A. Residual variances and covariance estimates for the best model (2 temporal and 2 spatial groups). Years and salinity zone columns indicate the group for which the variance or covariance was estimated, the variable column shows the variable for which covariance or residual variances were estimated. For covariances, the other variable name is shown in the covariance variable column. SE is the standard error associated with the estimate, and Lower/Upper 95% CI are the lower and upper approximate 95% confidence intervals, respectively. Exogeneous variables (temperature and salinity) do not have estimates of error.

Years	Salinity Zone	Variable	Co-variance Variable	Estimate	SE	Lower 95% CI	Upper 95% CI
1991-2002	Low	Temperature		0.427	NA	NA	NA
1991-2002	Low	Temperature	Salinity	0.378	NA	NA	NA
1991-2002	Low	Salinity		5.710	NA	NA	NA
1991-2002	Low	MSX Prevalence		87.309	7.954	71.720	102.898
1991-2002	Low	Dermo Prevalence		578.255	52.678	475.007	681.503
1991-2002	Low	Mortality		204.373	18.618	167.882	240.864
2003-2017	Low	Temperature		0.525	NA	NA	NA
2003-2017	Low	Temperature	Salinity	0.177	NA	NA	NA
2003-2017	Low	Salinity		6.203	NA	NA	NA
2003-2017	Low	MSX Prevalence		7.023	0.548	5.950	8.096
2003-2017	Low	Dermo Prevalence		967.474	75.432	819.627	1115.320
2003-2017	Low	Mortality		147.718	11.517	125.144	170.292
1991-2002	Medium/High	Temperature		0.423	NA	NA	NA
1991-2002	Medium/High	Temperature	Salinity	0.536	NA	NA	NA
1991-2002	Medium/High	Salinity		7.343	NA	NA	NA
1991-2002	Medium/High	MSX Prevalence		242.481	21.864	199.628	285.333
1991-2002	Medium/High	Dermo Prevalence		314.795	28.384	259.162	370.428
1991-2002	Medium/High	Mortality		331.169	29.860	272.642	389.696
2003-2017	Medium/High	Temperature		0.468	NA	NA	NA
2003-2017	Medium/High	Temperature	Salinity	0.327	NA	NA	NA
2003-2017	Medium/High	Salinity		5.463	NA	NA	NA
2003-2017	Medium/High	MSX Prevalence		78.869	6.149	66.817	90.922
2003-2017	Medium/High	Dermo Prevalence		748.102	58.328	633.779	862.425
2003-2017	Medium/High	Mortality		112.985	8.809	95.719	130.251

Table 2-A. Years and NOAA codes where freshets were known to occur. Data from bars within these NOAA codes in the years listed were not included in the structural equation models.

Year	NOAA Code
1993	377
1994	377
1996	377
1998	377
1993	274
1994	129
1994	25
1994	331
1994	231
1994	337
1996	129
1996	25
1996	331
1996	231
1998	129
1998	337
2011	25

References

Abbe GR, McCollough CB, Barker LS, Dungan CF (2010) Performance of disease-tolerant strains of eastern oyster (*Crassostrea virginica)* in the Patuxent River, Maryland, 2003 to 2007. J Shellfish Res 29:161–175

Albright BW, Abbe GR, McCollough CB, Barker LS, Dungan CF (2007) Growth and mortality of dermo-disease-free juvenile oysters (*Crassostrea virginica*) at three salinity regimes in an enzootic area of Chesapeake Bay. J Shellfish Res 26:451–463

Andrews JD (1982) Epizootiology of late summer and fall infections of oysters by *Haplosporidium nelsoni*, and comparison to annual life cycle of *Haplosporidium costalis*, a typical haplosporidan. J Shellfish Res 2:15–23

Andrews JD, Hewatt WG (1957) Oyster mortality studies in Virginia. II. The fungus disease caused by *Dermocystidium marinum* in oysters of Chesapeake Bay. Ecol Monogr 27:1–25

Andrews JD, Wood JL (1967) Oyster mortality studies in Virginia. VI. History and distribution of *Minchinia nelsoni*, a pathogen of oysters, in Virginia. Chesap Sci 8:1–13

Arzul I, Carnegie RB (2015) New perspective on the haplosporidian parasites of molluscs. J Invertebr Pathol 131:32–42

Audemard C, Ragone-Calvo LM, Paynter KT, Reece KS, Burreson EM (2006) Real-time PCR investigation of parasite ecology: in situ determination of oyster parasite *Perkinsus marinus* transmission dynamics in lower Chesapeake Bay. Parasitology 132:827–842

Brooks EN, Deroba JJ (2015) When "data" are not data: the pitfalls of post hoc analyses that use stock assessment model output. Can J Fish Aquat Sci 72:634–641

Brown BL, Butt AJ, Meritt D, Paynter KT (2005a) Evaluation of resistance to dermo in eastern oyster strains tested in Chesapeake Bay. Aquac Res 36:1544–1554

Brown BL, Butt AJ, Shelton SW, Meritt D, Paynter KT (2005b) Resistance of dermo in eastern oysters, *Crassostrea virginica* (Gmelin), of North Carolina but not Chesapeake Bay heritage. Aquac Res 36:1391–1399

Burge CA, Mark Eakin C, Friedman CS, Froelich B, Hershberger PK, Hofmann EE, Petes LE, Prager KC, Weil E, Willis BL, Ford SE, Harvell CD (2014) Climate change influences on marine infectious diseases: Implications for management and society. Ann Rev Mar Sci 6:249–277

Burnham K, Anderson D (2002) Model selection and multimodel inference: A practical information-theoretic approach. Springer-Verlag NewYork, Inc., New York

Burreson EM (1991) Effects of *Perkinsus marinus* infection in the eastern oyster, *Crassostrea virginica*: I. Susceptibility of native and MSX-resistant stocks. J Shellfish Res 10:417–423

Burreson EM, Ragone-Calvo LM (1996) Epizootiology of *Perkinsus marinus* disease of oysters in Chesapeake Bay, with emphasis on data since 1985. J Shellfish Res 15:17–34

Bushek D, Allen S (1996) Host-parasite interactions among broadly distributed populations of the eastern oyster *Crassostrea virginica* and the protozoan *Perkinsus marinus*. Mar Ecol Prog Ser 139:127–141

Bushek D, Ford SE (2016) Anthropogenic impacts on an oyster metapopulation: Pathogen introduction, climate change and responses to natural selection. Elem Sci Anthr 4:1–13

Bushek D, Ford SE, Burt I (2012) Long-term patterns of an estuarine pathogen along a salinity gradient. J Mar Res 70:225–251

Bushek D, Ford SE, Chintala MM (2002) Comparison of in vitro-cultured and wild-type *Perkinsus marinus*. III. Fecal elimination and its role in transmission. Dis Aquat Organ 51:217–225

Caddy JF (1989) A perspective on the population dynamics and assessment of scallop fisheries, with special reference to the sea scallop, *Placopecten megellanicus* Gmelin. In: Marine invertebrate fisheries: Their assessment and management.p 559–589

Carnegie RB, Burreson EM (2011) Declining impact of an introduced pathogen: *Haplosporidium nelsoni* in the oyster *Crassostrea virginica* in Chesapeake Bay. Mar Ecol Prog Ser 432:1–15

Carriker MR, Gaffney PM (1996) A catalogue of selected species of living oysters (Ostreacea) of the world. In: eastern oyster *Crassostrea virginica*. Maryland Sea Grant College, University of Maryland System, College Park, p 1–18

Chai AL, Homer ML, Tsai CF, Goulletquer P (1992) Evaluation of oyster sampling efficiency of patent tongs and an oyster dredge. North Am J Fish Manag 12:825–832

Christmas JF, McGrinty MR, Randle DA, Smith GF, Jordan SJ (1997) Oyster shell disarticulation in three Chesapeake Bay tributaries. J Shellfish Res 16:115–123

Chu F-LE, Peyre JF La (1993) *Perkinsus marinus* susceptibility and defense-related activities in eastern oysters *Crassostrea virginica*: temperature effects. Dis Aquat Organ 16:223–234

Chu F-LE, Peyre JF La, Burreson CS (1993) *Perkinsus marinus* infection and potential defense-related activities in eastern oysters, *Crassostrea virginica*: Salinity effects. J Invertebr Pathol 62:226–232

Clark WG (1999) Effects of an erroneous natural mortality rate on a simple age-structured stock assessment. Can J Fish Aquat Sci 56:1721–1731

Deroba JJ, Schueller AM (2013) Performance of stock assessments with misspecified age- and time-varying natural mortality. Fish Res 146:27–40

Dickie LM (1955) Fluctuations in abundance of the giant scallop, *Placopecten magellanicus* (Gmelin), in the Digby area of the Bay of Fundy. J Fish Board Canada 12:797–857

Encomio VG, Stickler SM, Allen SKJ, Chu FL (2005) Performance of "natural dermo-resistant" oyster stocks-survival, disease, growth, condition and energy reserves. J Shellfish Res 24:143–156

Farley CA (1967) A proposed life cycle of *Minchinia nelsoni* (Haplosporida, Haplosporidiidae) in the American oyster *Crassostrea virginica*. J Protozool 14:616–625

Farley CA (1968) *Minchinia nelsoni* (Haplosporida) disease syndrome in the American oyster *Crassostrea virginica*. J Protozool 15:585–599

Ford SE (1985) Effects of salinity on survival of the MSX parasite *Haplosporidium nelsoni* (Haskin, Stuuber, and Mackin) in oysters. J Shellfish Res 5:85–90

Ford SE, Bushek D (2012) Development of resistance to an introduced marine pathogen by a native host. J Mar Res 70:205–223

Ford S, Cummings M, Powell EN (2006) Estimating mortality in natural assemblages of oysters. Estuaries and Coasts 29:361–374

Ford SE, Haskin HH (1982) History and epizootiology of *Haplosporidium nelsoni* (MSX), an oyster pathogen in Delaware Bay, 1957–1980. J Invertebr Pathol 40:118–141

Ford S, Powell E, Klinck J, Hofmann E (1999) Modeling the MSX parasite in eastern oyster (*Crassostrea virginica*) populations. I. Model development, implementation, and verification. J Shellfish Res 18:475–500

Ford SE, Scarpa E, Bushek D (2012) Spatial and temporal variability of disease refuges in an estuary: Implications for the development of resistance. J Mar Res 70:253–277

Ford SE, Tripp MR (1996) Diseases and defense mechanisms. In: The eastern oyster *Crassostrea virginica*. Maryland Sea Grant College, University of Maryland System, College Park, p 581–660

Frank-Lawale A, Allen SK, Dégremont L (2014) Breeding and domestication of eastern oyster (*Crassostrea virginica*) lines for culture in the Mid-Atlantic, USA: Line development and mass selection for disease resistance. J Shellfish Res 33:153–165

Gauthier DT, Latour RJ, Heisey DM, Bonzek CF, Gartland J, Burge EJ, Vogelbein WK (2008) Mycobacteriosis-associated mortality in wild striped bass (*Morone saxatilis*) from Chesapeake Bay, USA. Ecol Appl 19:1718–1727

Gelman A, Rubin DB (1992) Inference from iterative simulation using multiple sequences. Stat Sci 7:457–472

Gulka G., Chang PW., Marti KA (1983) Prokaryotic infection associated with a mass mortality of the sea scallop, *Placopecten magellanicus*. J Fish Dis 6:355–364

Hannan EJ, Quinn BG (1979) The determination of the order of an autoregression. J R Stat Soc Ser B 41:190–195

Harvell CD, Mitchell CE, Ward JR, Alter S, Dobson AP, Ostfeld RS, Samuel MD (2002) Climate warming and disease risks for terrestrial and marine biota. Science 296:2158–2162

Haskin HH, Ford SE (1979) Development of resistance to *Minchinia nelsoni* (MSX) mortality in laboratory-reared and native oyster stocks in Delaware Bay. Mar Fish Rev 41:54–63

Haskin HH, Ford SE (1982) *Haplosporidium nelsoni* (MSX) on Delaware Bay seed oyster beds: A host-parasite relationship along a salinity gradient. J Invertebr Pathol 40:388–405

Hewatt WG, Andrews JD (1956) Temperature control experiments on the fungus disease, *Dermocystidium marinum*, of oysters. Proc Natl Shellfish Assoc 46:129–133

Hewitt DA, Hoenig JM (2005) Comparison of two approaches for estimating natural mortality based on longevity. Fish Bull 103:433–437

Hiemstra PH, Pebesma EJ, Twenhöfel CJW, Heuvelink GBM (2009) Real-time automatic interpolation of ambient gamma dose rates from the Dutch radioactivity monitoring network. Comput Geosci 35:1711–1721

Hoenig JM (1983) Empirical use of longevity data to estimate mortality rates. Fish Bull 81:898–903

Hoenig JM, Groner ML, Smith MW, Vogelbein WK, Taylor DM, Landers DF, Swenarton JT, Gauthier DT, Sadler P, Matsche MA, Haines AN, Small HJ, Pradel R, Choquet R, Shields JD (2017) Impact of disease on the survival of three commercially fished species. Ecol Appl 27:2116–2127

Holmes EE, Ward EJ, Scheuerell MD (2018) Analysis of multivariate time-series using the MARSS package. Seattle, WA

Holmes E, Ward E, Wills K (2012) MARSS: Mulitivariate autoregressive state-space modeling. R J 4:11–19

Johnson KF, Monnahan CC, Mcgilliard CR, Vert-pre KA, Anderson SC, Cunningham CJ, Hurtado-Ferro F, Licandeo RR, Muradian ML, Ono K, Szuwalski CS, Valero JL, Whitten AR, Punt AE (2015) Time-varying natural mortality in fisheries stock assessment models: identifying a default approach. ICES J Mar Sci 72:137–150

Kellogg ML, Cornwell JC, Owens MS, Paynter KT (2013) Denitrification and nutrient assimilation on a restored oyster reef. Mar Ecol Prog Ser 480:1–19

Kenchington TJ (2014) Natural mortality estimators for information-limited fisheries. Fish Fish 15:533–562

Kennedy VS, Breisch LL (1983) Sixteen decades of political management of the oyster fishery in Maryland's Chesapeake Bay. J Environ Manage 164:153–171

Kuha J (2004) AIC and BIC: Comparisons of assumptions and performance. Sociol Methods Res 33:188–229

Mackin JG (1956) *Dermocystidium marinum* and salinity. Proc Natl Shellfish Assoc 46:116–128

Mann R, Powell EN (2007) Why oyster restoration goals in the Chesapeake Bay are not and probably cannot be achieved. J Shellfish Res 26:905–917

Marenghi F, Ashton-Alcox K, Wong R, Reynolds B, Ozbay G (2017) Dredge efficiency on natural oyster grounds in Delaware Bay and its application in monitoring the eastern oyster (*Crassostrea virginica*) stock in Delaware, USA. Fish Res 186:292–300

Marty GD, Hulson PJF, Miller SE, Quinn TJ, Moffitt SD, Merizon RA (2010) Failure of population recovery in relation to disease in Pacific herring. Dis Aquat Organ 90:1–14

Marty GD, Quinn TJII, Carpenter G, Meyers TR, Willits NH (2003) Role of disease in abundance of a Pacific herring (*Clupea pallasi*) population. Can J Fish Aquat Sci 60:1258–1265

Maryland Department of Natural Resources (2001) Maryland oyster population status report: 1996-2000 fall surveys. Annapolis, MD

Maryland Department of Natural Resources (2016) Oyster management review: 2010-2015. Annapolis, MD

Maryland Department of Natural Resources (2018) A stock assessment of the eastern oyster, *Crassostrea virginica*, in the Maryland waters of Chesapeake Bay. Annapolis, MD

Messerman NA, Bowden TJ (2016) Survey of potential reservoir species for the oyster parasite multinucleate sphere X (*Haplosporidium nelsoni*) in and around oyster farms in the Damariscotta River Estuary, Maine. J Shellfish Res 35:851–856

Morson JM, Munroe DM, Ashton-Alcox KA, Powell EN, Bushek D, Gius J (2018) Density-dependent capture efficiency of a survey dredge and its influence on the stock assessment of eastern oysters (*Crassostrea virginica*) in Delaware Bay. Fish Res 205:115–121

Munroe DM, Powell EN, Ford SE, Hofmann EE, Klinck JM (2015) Outcomes of asymmetric selection pressure and larval dispersal on evolution of disease resistance: A metapopulation modeling study with oysters. Mar Ecol Prog Ser 531:221–239

Munroe D, Tabatabai A, Burt I, Bushek D, Powell EN, Wilkin J (2013) Oyster mortality in Delaware Bay: Impacts and recovery from Hurricane Irene and Tropical Storm Lee. Estuar Coast Shelf Sci 135:209–219

Murphy RR, Curriero FC, Ball WP (2010) Comparison of spatial interpolation methods for water quality evaluation in the Chesapeake Bay. J Environ Eng 136:160–171

Newell RIE (1988) Ecological changes in Chesapeake Bay: Are they the result of overharvesting the american oyster, *Crassostrea virginica*? In: Understanding the estuary: Advances in Chesapeake Bay research.p 536–546

Newell RIE, Kemp WM, Hagy JD, Cerco CF, Testa JM, Boynton WR (2007) Top-down control of phytoplankton by oysters in Chesapeake Bay, USA: Comment on Pomeroy et al. (2006). Mar Ecol Prog Ser 341:293–298

Paraso MC, Ford SE, Powell EN, Hofmann EE, Klinck JM (1999) Modeling the MSX parasite in eastern oyster (*Crassostrea virginica*) populations. II. Salinity effects. J Shellfish Res 18:501–516

Pauly D (1980) On the interrelationships between natural mortality, growth parameters, and mean environmental temparature in 175 fish stocks. ICES J Mar Sci 39:175–192

Peterson CD, Belcher CN, Bethea DM, Driggers WBI, Frazier BS, Latour RJ (2017) Preliminary recovery of coastal sharks in the south-east United States. Fish Fish 18:845–859

Petes LE, Brown AJ, Knight CR (2012) Impacts of upstream drought and water withdrawals on the health and survival of downstream estuarine oyster populations. Ecol Evol 2:1712–1724

Peyre MK La, Gossman B, Peyre JF La (2009) Defining optimal freshwater flow for oyster production: Effects of freshet rate and magnitude of change and duration on eastern oysters and *Perkinsus marinus* infection. Estuaries and Coasts 32:522–534

Peyre MK La, Nickens AD, Volety AK, Tolley GS, Peyre JF La (2003) Environmental significance of freshets in reducing *Perkinsus marinus* infection in eastern oysters *Crassostrea virginica*: Potential management applications. Mar Ecol Prog Ser 248:165–176

Pollack JB, Kim HC, Morgan EK, Montagna PA (2011) Role of flood disturbance in natural oyster (*Crassostrea virginica*) population maintenance in an estuary in South Texas, USA. Estuaries and Coasts 34:187–197

Powell EN, Ashton-Alcox KA, Kraeuter JN (2007) Reevaluation of eastern oyster dredge efficiency in survey mode: Application in stock assessment. North Am J Fish Manag 27:492–511

Powell EN, Klinck JH, Ford SE, Hofmann EE, Jordan SJ (1999) Modeling the MSX parasite in eastern oyster (*Crassostrea virginica*) populations. III. Regional application and the problem of transmission. J Shellfish Res 18:517–537

Powell EN, Klinck JM, Guo X, Ford SE, Bushek D (2011) The potential for oysters, *Crassostrea virginica*, to develop resistance to dermo disease in the field: Evaluation using a gene-based population dynamics model. J Shellfish Res 30:685–712

Powell EN, Klinck JM, Guo X, Hofmann EE, Ford SE, Bushek D (2012) Can oysters *Crassostrea virginica* develop resistance to dermo disease in the field: The impediment posed by climate cycles. J Mar Res 70:309–355

Ragone Calvo LM, Dungan CF, Roberson BS, Burreson EM (2003) Systematic evaluation of factors controlling *Perkinsus marinus* transmission dynamics in lower Chesapeake Bay. Dis Aquat Organ 56:75–86

Rodney WS, Paynter KT (2006) Comparisons of macrofaunal assemblages on restored and non-restored oyster reefs in mesohaline regions of Chesapeake Bay in Maryland. J Exp Mar Bio Ecol 335:39–51

Rosseel Y (2012) lavaan: An R package for structural equation modeling. J Stat Softw 48:1–36

Shumway SE (1996) Natural environmental factors. In: The eastern oyster *Crassostrea virginica*. Maryland Sea Grant College, University of Maryland System, College Park, p 467–513

Stan Development Team (2018) RStan: The R interface to Stan.

Sunila I, Karolus J, Lang EP, Mroczka ME, Volk J (2000) Transmission of the haplosporidian parasite MSX *Haplosporidium nelsoni* to the eastern oyster *Crassostrea virginica* in an upweller system. Dis Aquat Organ 42:153–155

Tarnowski M (2012) Maryland oyster population status report: 2011 fall survey. Annapolis, MD

Tarnowski M (2016) Maryland oyster population status report: 2015 fall survey. Annapolis, MD

Tarnowski M (2017) Maryland oyster population status report: 2016 fall survey. Annapolis, MD

Thompson SK (2002) Sampling. Wiley, New York.

Vølstad JH, Dew J, Tarnowski M (2008) Estimation of annual mortality rates for eastern oysters (*Crassostrea virginica*) in Chesapeake Bay based on box counts and application of those rates to project population growth of *C. virginica* and *C. ariakensis*. J Shellfish Res 27:525–533

Walter J, Hoenig JM, Wood RJ, Marti K (2007) An estimator of episodic mortality in bivalves with an application to sea scallops (*Placopecten magellanicus*). Fish Res 86:85–91

Wang Z, Haidvogel DB, Bushek D, Ford SE, Hofmann EE, Powell EN, Wilkin J (2012) Circulation and water properties and their relationship to the oyster disease MSX in Delaware Bay.

Ward JR, Lafferty KD (2004) The elusive baseline of marine disease: Are diseases in ocean ecosystems increasing? PLoS Biol 2:542–547

White ME, Wilson EA (1996) Predators, pests, and competitors. In: The eastern oyster *Crassostrea virginica*. Maryland Sea Grant College, University of Maryland System, College Park, p 559–580

Wilberg MJ, Livings ME, Barkman JS, Morris BT, Robinson JM (2011) Overfishing, disease, habitat loss, and potential extirpation of oysters in upper Chesapeake Bay. Mar Ecol Prog Ser 436:131–144

Yu H, He Y, Wang X, Zhang Q, Bao Z, Guo X (2011) Polymorphism in a serine protease inhibitor gene and its association with disease resistance in the eastern oyster (*Crassostrea virginica* Gmelin). Fish Shellfish Immunol 30:757–762

Zuur AF, Tuck ID, Bailey N (2003) Dynamic factor analysis to estimate common trends in fisheries time series. Can J Fish Aquat Sci 60:542–552